

¹ **Title:** Carbon cycling in mature and regrowth forests globally: a macroecological synthesis based on the
² global Forest Carbon (ForC) database

³ **Authors:**

⁴ Kristina J. Anderson-Teixeira^{1,2*}

⁵ Valentine Herrmann¹

⁶ Becky Banbury Morgan³

⁷ Ben Bond-Lamberty⁴

⁸ Susan C. Cook-Patton⁵

⁹ Abigail E. Ferson^{1,6}

¹⁰ Jennifer C. McGarvey¹

¹¹ Helene C. Muller-Landau¹

¹² Maria M. H. Wang^{1,7}

¹³ **Author Affiliations:**

¹⁴ 1. Conservation Ecology Center; Smithsonian Conservation Biology Institute; National Zoological Park,
¹⁵ Front Royal, VA 22630, USA

¹⁶ 2. Center for Tropical Forest Science-Forest Global Earth Observatory; Smithsonian Tropical Research
¹⁷ Institute; Panama, Republic of Panama

¹⁸ 3. School of Geography, University of Leeds, Leeds, UK

¹⁹ 4. Joint Global Change Research Institute, Pacific Northwest National Laboratory, College Park
²⁰ Maryland 20740, USA

²¹ 5. The Nature Conservancy; Arlington VA 22203, USA

²² 6. College of Natural Resources, University of Idaho; Moscow, Idaho 83843, USA

²³ 7. Grantham Centre for Sustainable Futures and Department of Animal and Plant Sciences, University of
²⁴ Sheffield, Western Bank, Sheffield, South Yorkshire S10 2TN, UK

²⁵ *corresponding author: teixeirak@si.edu; +1 540 635 6546

²⁶ ## [1] 0

²⁷ **NOTES TO COAUTHORS:**

²⁸ • We're still finalizing the data (and adding some data). Outliers in plots will all be checked/ resolved,
²⁹ and we'll be able to pull in more data (*GROA* needs classification by dominant vegetation before it can
³⁰ be pulled in, and we're working on that)

³¹ • “????” indicates a reference that we have entered in the .Rmd file, but not yet in the bibliography file.
³² Don't worry about those. (However, places with “REF” need references)

³³ • bold/ italic text indicates places where I know we need to go back and revisit/ fill in info

³⁴ **Summary**

³⁵ *Background.* Earth's climate is closely linked to forests, which strongly influence atmospheric carbon dioxide
³⁶ (CO_2) and climate by their impact on the global carbon (C) cycle. However, efforts to incorporate forests
³⁷ into climate models and CO_2 accounting frameworks have been constrained by a lack of accessible,
³⁸ global-scale data on how C cycling varies across forest types and stand ages.

³⁹ *Methods/Design.* Here, we draw from the Global Forest Carbon Database, ForC, to provide a macroscopic
⁴⁰ overview of C cycling in the world's forests, giving special attention to stand age-related variation.

⁴¹ Specifically, we use 12124 *ForC* records from 869 geographic locations representing 34 C cycle variables to
⁴² characterize ensemble C budgets for four broad forest types (tropical broadleaf evergreen, temperate
⁴³ broadleaf, temperate conifer, and taiga), including estimates for both mature and regrowth (age <100 years)
⁴⁴ forests. For regrowth forests, we quantify age trends for all variables.

⁴⁵ *Review Results/ Synthesis.* *ForC v3.0* yielded a fairly comprehensive picture of C cycling in the world's
⁴⁶ major forest biomes, with broad closure of C budgets. The rate of C cycling generally increased from boreal
⁴⁷ to tropical regions in both mature and regrowth forests, whereas C stocks showed less directional variation.
⁴⁸ The majority of flux variables, together with most live biomass pools, increased significantly with stand age,
⁴⁹ and the rate of increase again tended to increase from boreal to tropical regions.

⁵⁰ *Discussion.* NEED TO WRITE THIS!!!

⁵¹ *Key words:* forest ecosystems; carbon cycle; stand age; productivity; respiration; biomass; global

52 **Background**

53 Forest ecosystems are shaping the course of climate change (IPCC1.5) through their influence on atmospheric
54 carbon dioxide (CO₂). Despite the centrality of forest C cycling in regulating atmospheric CO₂, important
55 uncertainties in climate models (???, ???, ???, Krause *et al* 2018) and CO₂ accounting frameworks (Pan *et*
56 *al* 2011) can be traced to lack of accessible, comprehensive data on how C cycling varies across forest types
57 and in relation to stand history. These require large-scale databases with global coverage, which runs
58 contrary to the nature in which forest C stocks and fluxes are measured and published. While remote sensing
59 measurements are increasingly useful for global- or regional-scale estimates of a few critical variables [e.g.,
60 aboveground biomass: (???); **REF**; gross primary productivity, *GPP*: Li and Xiao (2019); **REFS for**
61 **biomass change, net CO2 flux**], measurement of most forest C stocks and fluxes require intensive
62 on-the-ground data collection. Here, we provide a robust and comprehensive analysis of carbon cycling from
63 a stand to global level, and by biome and stand age, using the largest global compilation of forest carbon
64 data, which is available in our open source Global Carbon Forest database (ForC; Fig. 1).

65 A robust understanding of forest impacts on global C cycling is essential. Annual gross CO₂ sequestration in
66 forests (gross primary productivity, *GPP*) is estimated at >69 Gt C yr⁻¹ (???), or >7 times average annual
67 fossil fuel emissions from 2009-2018 (9.5 ± 0.5 Gt C yr⁻¹; ???). Most of this enormous C sequestration is
68 counterbalanced by CO₂ releases to the atmosphere through ecosystem respiration (*R_{eco}*) or fire, with forests
69 globally dominant as sources of both soil respiration (???) and fire emissions (REF). (check if
70 **deforestation statistic below includes natural fire, exclude here if it does.**) In recent years, the
71 remaining CO₂ sink averaged 3.2 ± 0.6 GtC yr⁻¹ from 2009-2018, offsetting 29% of anthropogenic fossil fuel
72 emissions (???). Yet, this sink is reduced by *deforestation/ forest losses to anthropogenic and natural*
73 *disturbances*. Recent net deforestation (*i.e.*, gross deforestation minus regrowth) has been a source of CO₂
74 emissions, estimated at ~1.1 Gt C yr⁻¹ from YEAR-YEAR (Pan *et al* 2011; **UPDATE**), reducing the net
75 forest sink to ~1.1-2.2 Gt C yr⁻¹ across Earth's forests (???).

76 The future of the current forest C sink is dependent both upon forest responses to climate change itself and
77 human land use decisions, which will feedback and strongly influence the course of climate change.
78 Regrowing forests in particular will play an important role (Pugh *et al* 2019), as these represent a large
79 (~#%) and growing proportion of Earth's forests (McDowell *et al* 2020). Understanding, modeling, and
80 managing forest-atmosphere CO₂ exchange is thus central to efforts to mitigate climate change [Grassi *et al*
81 (2017); Griscom *et al* (2017); **Cavaleri et al 2015**].

82 Despite the importance of forests, comprehensive global studies have historically been limited by the scattered
83 and more local nature of research studies. Primary research articles typically cover only a small numbers of
84 sites at a time. The rare exceptions that span regions or continents with rare exceptions spanning regions or
85 continents are typically coordinated through research networks such as ForestGEO (Anderson-Teixeira *et al*
86 2015, e.g., Lutz *et al* 2018) or FLUXNET [Baldocchi *et al* (2001); e.g., **FLUXNET_REF**]. The result of
87 decades of research on forest C cycling is that tens of thousands of records have been distributed across
88 literally thousands of scientific articles –often behind paywalls– along with variation in data formats, units,
89 measurement methods, *etc..* In this format, the data are effectively inaccessible for many global-scale
90 analyses, including those attempting to benchmark model performance with global data (Clark *et al* 2017,
91 Luo *et al* 2012), quantify the the role of forests in the global C cycle (*e.g.*, Pan *et al* 2011), or use
92 book-keeping methods to quantify actual or scenario-based exchanges of CO₂ between forests and the
93 atmosphere [Griscom *et al* (2017); **REFS**]. Scattered data are not conducive for advancing science nor for

making decisions about how to best manage our forests as a tool for constraining the climate crisis.

To address the need for global-scale analyses of forest C cycling, we recently developed *ForC* (Anderson-Teixeira *et al* 2016, pp @anderson-teixeira_forc_2018). *ForC* contains published estimates of forest ecosystem C stocks and annual fluxes (>50 variables), with the different variables capturing the unique ecosystem pools (e.g., woody, foliage, and root biomass; dead wood) and flux types (e.g, gross and net primary productivity; soil, root, and ecosystem respiration). These data are ground-based measurements, and *ForC* contains associated data required for interpretation (e.g., stand history, measurement methods). These data have been amalgamated from original peer-reviewed publications, either directly or via intermediary data compilations. Since its most recent publication (Anderson-Teixeira *et al* 2018), *ForC* has grown to include two additional large databases: the Global Soil Respiration Database (SRDB; Bond-Lamberty and Thomson 2010) and the Global Reforestation Opportunity Assessment database (GROA; Cook-Patton *et al* 2020) that also synthesized published forest C data. Following these additions, *ForC* currently contains 47837 records from 10609 plots and 1532 distinct geographic areas representing all forested biogeographic and climate zones. This represents an 175% increase in records from the prior publication (Anderson-Teixeira *et al* 2018).

Here, we analyze the more extensive *ForC* data (Fig. 1) to provide a robust overview of stand-level carbon cycling of the world's major forest biomes and how it varies with stand age. Our primary goal is to provide a data-driven summary of our current state of knowledge on broad trends in forest C cycling. Specifically, we address three broad questions:

1. How thoroughly can we represent C budgets for each of the world's major forest biomes (*i.e.*, tropical, temperate broadleaf and deciduous, boreal) based on the current *ForC* data?
2. How do C cycling vary across the world's major forest biomes?
3. How does C cycling vary with stand age (in interaction with biome)?

While components of these questions have been previously addressed (Luyssaert *et al* 2007, Anderson-Teixeira *et al* 2016, Cook-Patton *et al* 2020, Banbury Morgan *et al* n.d.), our analysis represents by far the most comprehensive analysis of C cycling in global forests, and will serve as a foundation for improved understanding of global forest C cycling and highlight where key sources of uncertainty still reside.

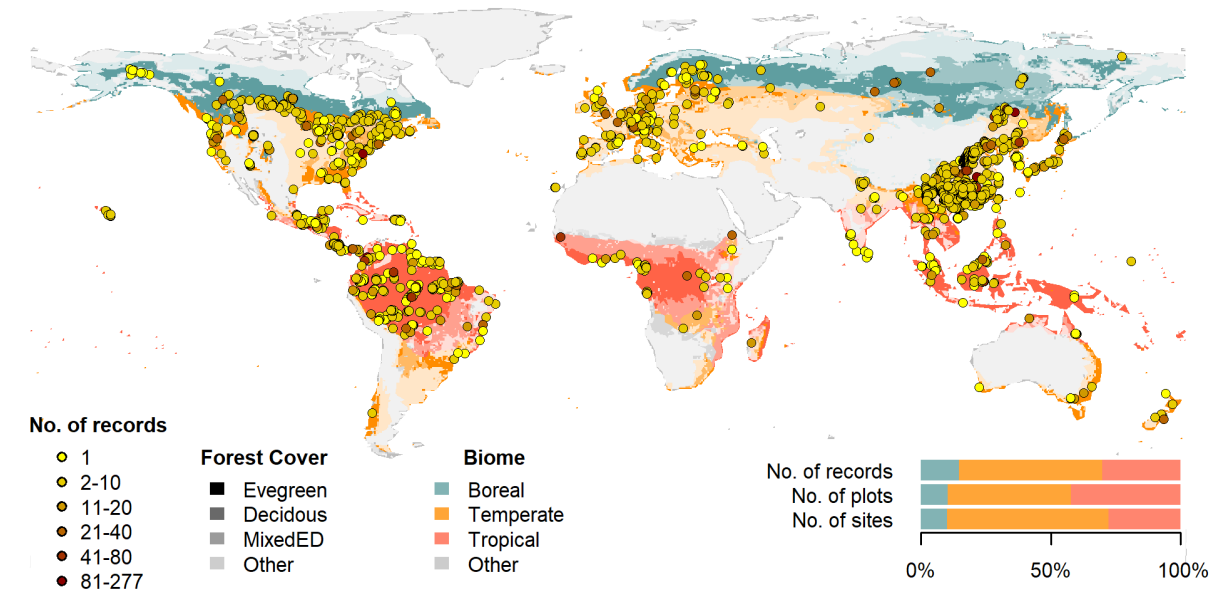


Figure 1 | Map of sites included in this analysis. Symbols are colored according to the number of records at each site. Underlying map shows coverage of evergreen, deciduous, and mixed forests (from SYNMAP; Jung et al. 2006) and biomes. Distribution of sites, plots, and records among biomes is shown in the inset.

121 Methods/ Design

122 This review synthesizes data from the *ForC* database (Fig. 1; <https://github.com/forc-db/ForC>;
 123 Anderson-Teixeira *et al* 2016, pp @anderson-teixeira_forc_2018). *ForC* amalgamates numerous
 124 intermediary data sets (*e.g.*, Luyssaert *et al* 2007, Bond-Lamberty and Thomson 2010, Cook-Patton *et al*
 125 2020) and original studies. Original publications were referenced to check values and obtain information not
 126 contained in intermediary data sets, although this process has not been completed for all records. The
 127 database was developed with goals of understanding how C cycling in forests varies across broad geographic
 128 scales and as a function of stand age. As such, there has been a focus on incorporating data from regrowth
 129 forests (*e.g.*, Anderson *et al* 2006, Martin *et al* 2013, Bonner *et al* 2013) and obtaining stand age data when
 130 possible (83% of records in v.2.0; Anderson-Teixeira *et al* 2018). Particular attention was given to developing
 131 the database for tropical forests (Anderson-Teixeira *et al* 2016), which represented roughly one-third of
 132 records in *ForC* v.2.0* (Anderson-Teixeira *et al* 2018). Since publication of *ForC* v.2.0, we added the
 133 following data to *ForC*: the Global Database of Soil Respiration Database (*SRDB* v.##, 9488 records;
 134 Bond-Lamberty and Thomson 2010), the Global Reforestation Opportunity Assessment database (*GROA*
 135 v1.0, 18143 records; Cook-Patton *et al* 2020, Anderson-Teixeira *et al* 2020). We've also added data from
 136 individual publications (detailed list at [https://github.com/forc-
 137 db/ForC/blob/master/database_management_records/ForC_data_additions_log.csv](https://github.com/forc-db/ForC/blob/master/database_management_records/ForC_data_additions_log.csv)), with a particular
 138 focus on productivity (Banbury Morgan *et al* n.d., *e.g.*, Taylor *et al* 2017), dead wood, and ForestGEO sites
 139 (*e.g.*, Lutz *et al* 2018, p @johnson_climate_2018). We note that there remains a significant amount of
 140 relevant data that is not yet included in *ForC*, particularly biomass data from national forest inventories

141 (e.g.,; **REFS**). The database version used for this analysis has been tagged as a new release on Github (**XX**)
142 and assigned a DOI through Zenodo (DOI: TBD).

143 To facilitate analyses, we created a simplified version of ForC, *ForC-simplified*
144 (https://github.com/forc-db/ForC/blob/master/ForC_simplified), which we analyzed here. In generating
145 *ForC-simplified*, all measurements originally expressed in units of dry organic matter (*OM*) were converted
146 to units of C using the IPCC default of $C = 0.47 * OM$ (IPCC 2006). Duplicate or otherwise conflicting
147 records were reconciled as described in APPENDIX S1, resulting in a total of 32746 records (68.5% size of
148 total database). Records were filtered to remove plots that had undergone significant anthropogenic
149 management or major disturbance since the most recent stand initiation event. Specifically, we removed all
150 plots flagged as managed in ForC-simplified (18.7%). This included plots with any record of managements
151 manipulating CO₂, temperature, hydrology, nutrients, or biota, as well as any plots whose site or plot name
152 contained the terms “plantation”, “planted”, “managed”, “irrigated”, or “fertilized”. Plots flagged as
153 disturbed in ForC-simplified (5.6%) included stands that had undergone any notable anthropogenic thinning
154 or partial harvest. We retained sites that were grazed or had undergone low severity natural disturbances
155 (<10% mortality) including droughts, major storms, fires, and floods. We removed all plots for which no
156 stand history information had been retrieved (7.3%). In total, this resulted in 23448 records (49% of the
157 records in the database) being eligible for inclusion in the analysis.

158 We selected 23 annual flux and 11 C stock variables for inclusion in the analysis. These different flux and
159 stock variables (Table 1) represent different pools (e.g., aboveground biomass, dead wood, ecosystem total)
160 and levels of combination (e.g., total aboveground net primary productivity (*ANPP*) versus the ANPP of
161 individual elements such as foliage, roots, and branches. Note that two flux variables, aboveground
162 heterotrophic (R_{het-ag}) and total (R_{het}) respiration, were included for conceptual completeness but had no
163 records in *ForC* (Table 1). Records for these variables represented 67.9% of the total records eligible for
164 inclusion. For this analysis, we combined some of ForC’s specific variables (e.g., multiple variables for net
165 primary productivity, such as measurements including or excluding fruit and flower production and herbivory)
166 into more broadly defined variables. Specifically, net ecosystem exchange (measured by eddy-covariance;
167 **FLUXNET REF**) and biometric estimates of *NEP* were combined into the single variable *NEP* (Table 1).
168 Furthermore, for *NPP*, *ANPP*, and *ANPP_{litterfall}*, *ForC* variables specifying inclusion of different
169 components were combined. Throughout ForC, for all measurements drawing from tree census data (e.g.,
170 biomass, productivity), the minimum diameter breast height (DBH) threshold for tree census was $\leq 10\text{cm}$.
171 All records were measured directly or derived from field measurements (as opposed to modeled).

172 For this analysis, we grouped forests into four broad biome types based on climate zones and dominant
173 vegetation type (tropical broadleaf, temperate broadleaf, temperate needleleaf, and boreal needleleaf) and
174 two age classifications (young and mature). Climate zones (Fig. 1) were defined based on site geographic
175 coordinates according to Köppen-Geiger zones (Rubel and Kottek 2010). We defined the tropical biome as
176 including all equatorial (A) zones, temperate biomes as including all warm temperate (C) zones and warmer
177 snow climates (Dsa, Dsb, Dwa, Dwb, Dfa, and Dfb), and the boreal biome as including the colder snow
178 climates (Dsc, Dsd, Dwc, Dwd, Dfc, and Dfd). Any forests in dry (B) and polar (E) Köppen-Geiger zones
179 were excluded from the analysis. We defined leaf type (broadleaf / needleleaf) was based on descriptions in
180 original publications (prioritized) or values extracted from a global map based on satellite observations
181 (SYNMAP; ???). For young tropical forests imported from *GROA* but not yet classified by leaf type, we
182 assumed that all were broadleaf, consistent with the rarity of naturally regenerating needleleaf forests in the

Table 1. Carbon cycle variables included in this analysis, their sample sizes, and summary of biome differences and age trends.

Variable	Description	N records			biome differences*	age trend†
		records	plots	geographic areas		
Annual fluxes						
<i>NEP</i>	net ecosystem production or net ecosystem exchange (+ indicates C sink)	329	146	88	n.s.	+; xB
<i>GPP</i>	gross primary production ($NPP + R_{auto}$ or $R_{eco} - NEE$)	303	115	84	$TrB > TeB \geq TeN \geq BoN$	+; xB
<i>NPP</i>	net primary production ($ANPP + BNPP$)	214	112	74	$TrB > TeB \geq TeN > BoN$	n.s.
<i>ANPP</i>	aboveground <i>NPP</i>	343	236	131	$TrB > TeB \geq TeN > BoN$	+; xB
<i>ANPP_{woody}</i>	woody production ($ANPP_{stem} + ANPP_{branch}$)	64	53	37	n.s.	+
<i>ANPP_{stem}</i>	woody stem production	217	190	117	$TrB > TeN \geq TeB \geq BoN$	n.s.
<i>ANPP_{branch}</i>	branch turnover	69	59	42	$TrB > TeB \geq TeN$	n.s.
<i>ANPP_{foliage}</i>	foliage production, typically estimated as annual leaf litterfall	162	132	88	$TrB > TeB \geq TeN > BoN$	+
<i>ANPP_{litterfall}</i>	litterfall, including leaves, reproductive structures, twigs, and sometimes branches	82	70	55	n.s.	+
<i>ANPP_{repro}</i>	production of reproductive structures (flowers, fruits, seeds)	51	44	34	-	-
<i>ANPP_{folivory}</i>	foliar biomass consumed by folivores	20	12	11	-	-
<i>M_{woody}</i>	woody mortality—i.e., B_{ag} of trees that die	18	18	18	-	-
<i>BNPP</i>	belowground NPP ($BNPP_{coarse} + BNPP_{fine}$)	148	116	79	$TrB > TeN \geq TeB \geq BoN$	+
<i>BNPP_{coarse}</i>	coarse root production	77	56	36	$TeN \geq TrB$	n.s.
<i>BNPP_{fine}</i>	fine root production	123	99	66	n.s.	+
<i>R_{eco}</i>	ecosystem respiration ($R_{auto} + R_{het}$)	213	98	70	$TrB > TeB \geq TeN$	+
<i>R_{auto}</i>	autotrophic respiration ($(R_{auto-ag} + R_{root})$)	24	23	15	-	-
<i>R_{auto-ag}</i>	aboveground autotrophic respiration (i.e., leaves and stems)	2	2	1	-	-
<i>R_{root}</i>	root respiration	181	139	95	$TrB \geq TeB$	+
<i>R_{soil}</i>	soil respiration ($R_{het-soil} + R_{root}$)	627	411	229	$TrB > TeB > TeN \geq BoN$	n.s.
<i>R_{het-soil}</i>	soil heterotrophic respiration	197	156	100	$TrB > TeB \geq TeN$	n.s.
<i>R_{het-ag}</i>	aboveground heterotrophic respiration	0	0	0	-	-
<i>R_{het}</i>	heterotrophic respiration ($(R_{het-ag} + R_{het-soil})$)	0	0	0	-	-
Stocks						
<i>B_{tot}</i>	total live biomass ($B_{ag} + B_{root}$)	188	157	87	$TrB \geq TeB > BoN$	+; xB
<i>B_{ag}</i>	aboveground live biomass ($B_{ag-wood} + B_{foliage}$)	4666	4272	625	$TrB \geq TeN \geq TeB > BoN$	+; xB
<i>B_{ag-wood}</i>	woody component of aboveground biomass	115	102	64	$TeN > TrB \geq BoN$	+; xB
<i>B_{foliage}</i>	foliage biomass	134	115	72	$TeN > TrB \geq BoN \geq TeB$	+; xB
<i>B_{root}</i>	total root biomass ($B_{root-coarse} + B_{root-fine}$)	2330	2299	361	n.s.	+; xB
<i>B_{root-coarse}</i>	coarse root biomass	134	120	73	$TeN > TeB \geq BoN$	+; xB
<i>B_{root-fine}</i>	fine root biomass	226	180	109	n.s.	+; xB
<i>DW_{tot}</i>	deadwood ($DW_{standing} + DW_{down}$)	79	73	42	-	+; xB
<i>DW_{standing}</i>	standing dead wood	36	35	22	-	-
<i>DW_{down}</i>	fallen dead wood, including coarse and sometimes fine woody debris	278	265	37	-	+; xB
<i>OL</i>	organic layer / litter/ forest floor	474	413	115	n.s.	+; xB

* Tr: Tropical, TeB: Temperate Broadleaf, TeN: Temperate Needleleaf, B: Boreal, n.s.: no significant differences

† + or -: significant positive or negative trend, xB: significant age x biome interaction, n.s.: no significant age trend

183 tropics (**REF**). We also classified forests as “young” (< 100 years) or “mature” (≥ 100 years or classified as
184 “mature”, “old growth”, “intact”, or “undisturbed” in original publication). Assigning stands to these
185 groupings required the exclusion of records for which *ForC* lacked geographic coordinates (0.4% of sites in
186 full database) or records of stand age (4.8% of records in full database). We also excluded records of stand
187 age = 0 year (0.8% of records in full database). In total, our analysis retained 76.2 of the focal variable
188 records for forests of known age. Numbers of records by biome and age class are given in Table S1.

189 Data were summarized to produce schematics of C cycling across the eight biome by age group combinations
190 identified above. To obtain the values reported in the C cycle schematics, we first averaged any repeated
191 measurements within a plot. Values were then averaged across geographically distinct areas, defined as plots
192 clustered within 25 km of one another (*sensu* Anderson-Teixeira *et al* 2018), weighting by area sampled if
193 available for all records. This step was taken to avoid pseudo-replication and to combine any records from
194 sites with more than one name in ForC.

195 We tested whether the C budgets described above “closed”—*i.e.*, whether they were internally consistent.
196 Specifically, we first defined relationships among variables: for example, $NEP = GPP - R_{eco}$,
197 $BNPP = BNPP_{coarse} + BNPP_{fine}$, $DW_{tot} = DW_{standing} + DW_{down}$. (**issue #44—but just delete**
198 **this chunk if not resolved before submission**) Henceforth, we refer to the variables on the left side of
199 the equation as “aggregate” fluxes or stocks, and those that are summed as “component” fluxes or stocks,
200 noting that the same variable can take both aggregate and component positions in different relationships.
201 We considered the C budget for a given relationship “closed” when component variables summed to within
202 one standard deviation of the aggregate variable.

203 To test for differences across mature forest biomes, we also examined how stand age impacted fluxes and
204 stocks, employing a mixed effects model [‘lmer’ function in ‘lme4’ R package version **x.xx**; **REF**] with biome
205 as fixed effect and plot nested within geographic.area as random effects on the intercept. When Biome had a
206 significant effect, we looked at a Tukey’s pairwise comparison to see which biomes were significantly different
207 from one another. This analysis was run for variables with records for at least seven distinct geographic areas
208 in more than one biome, excluding any biomes that failed this criteria (Table 1).

209 To test for age trends in young (<100yrs) forests, we employed a mixed effects model with biome and
210 $\log_{10}[\text{stand.age}]$ as fixed effects and plot nested within geographic.area as a random effect on the intercept.
211 This analysis was run for variables with records for at least three distinct geographic areas in more than one
212 biome, excluding any biomes that failed this criteria (Table 1). When the effect of stand age was significant
213 at $p \leq 0.05$ and when each biome had records for stands of at least 10 different ages, a biome \times stand.age
214 interaction was included in the model.

215 To facilitate the accessibility of our results and data, and to allow for rapid updates as additional data
216 become available, we have automated all database manipulation, analyses, and figure production in R
217 (**version, citation**).

218 Review Results/ Synthesis

219 Data Coverage

220 Of the 47837 records in *ForC* v3.0, 12124 met our strict criteria for inclusion in this study (Fig. 1). These
221 records were distributed across 5262 plots in 869 distinct geographic areas. Of the 23 flux and 11 stock

variables mapped in these diagrams, *ForC* contained sufficient mature forest data for inclusion in our statistical analyses (*i.e.*, records from ≥ 7 distinct geographic areas, and number of distinct plots < number of observations) for 20 fluxes and 9 stocks in tropical broadleaf forests, 15 fluxes and 8 stocks in temperate broadleaf forests, 14 fluxes and 7 stocks in temperate conifer forests, and 8 fluxes and 7 stocks in boreal forests. For regrowth forests (<100 yrs), *ForC* contained sufficient data for inclusion in our statistical analyses (*i.e.*, records from ≥ 3 distinct geographic areas, and number of distinct plots < number of observations) for 11 fluxes and 10 stocks in tropical broadleaf forests, 16 fluxes and 10 stocks in temperate broadleaf forests, 16 fluxes and 10 stocks in temperate conifer forests, and 14 fluxes and 9 stocks in boreal forests.

231 C cycling in mature forests

Average C cycles for mature tropical broadleaf, temperate broadleaf, temperate conifer, and boreal forests ≥ 100 years old and with no known major natural or anthropogenic disturbance are presented in Figures 2-5 (and available in tabular format in the *ForC* release accompanying this publication:

`ForC/numbers_and_facts/ForC_variable_averages_per_Biome.csv`.

For variables with records from ≥ 7 distinct geographic areas, these ensemble C budgets were generally consistent. *That is, component variables summed to within one standard deviation of their respective aggregate variables in all but two instances, both in temperate conifer forests (Fig. 5). (check all this with final results:*

https://github.com/forc-db/ForC/blob/master/numbers_and_facts/C_cycle_closure.csv,

and be sure to write out variable names at first occurrence, and provide a bit more detail)

For the temperate conifer biome, the average composite measure of aboveground biomass (B_{ag}) was less than the combined average value of woody biomass ($B_{ag-wood}$) and foliage biomass ($B_{foliage}$), partly due to the very high estimates of $B_{ag-wood}$. Within this biome, $B_{ag} < B_{ag-wood} + B_{foliage}$ and

$B_{root} < B_{root-coarse} + B_{root-fine}$ because $B_{ag-wood}$ and $B_{root-coarse}$ were very high, with strongly disproportionate numbers of records from the high-biomass forests of the US Pacific Northwest (Figs. S18, S21).

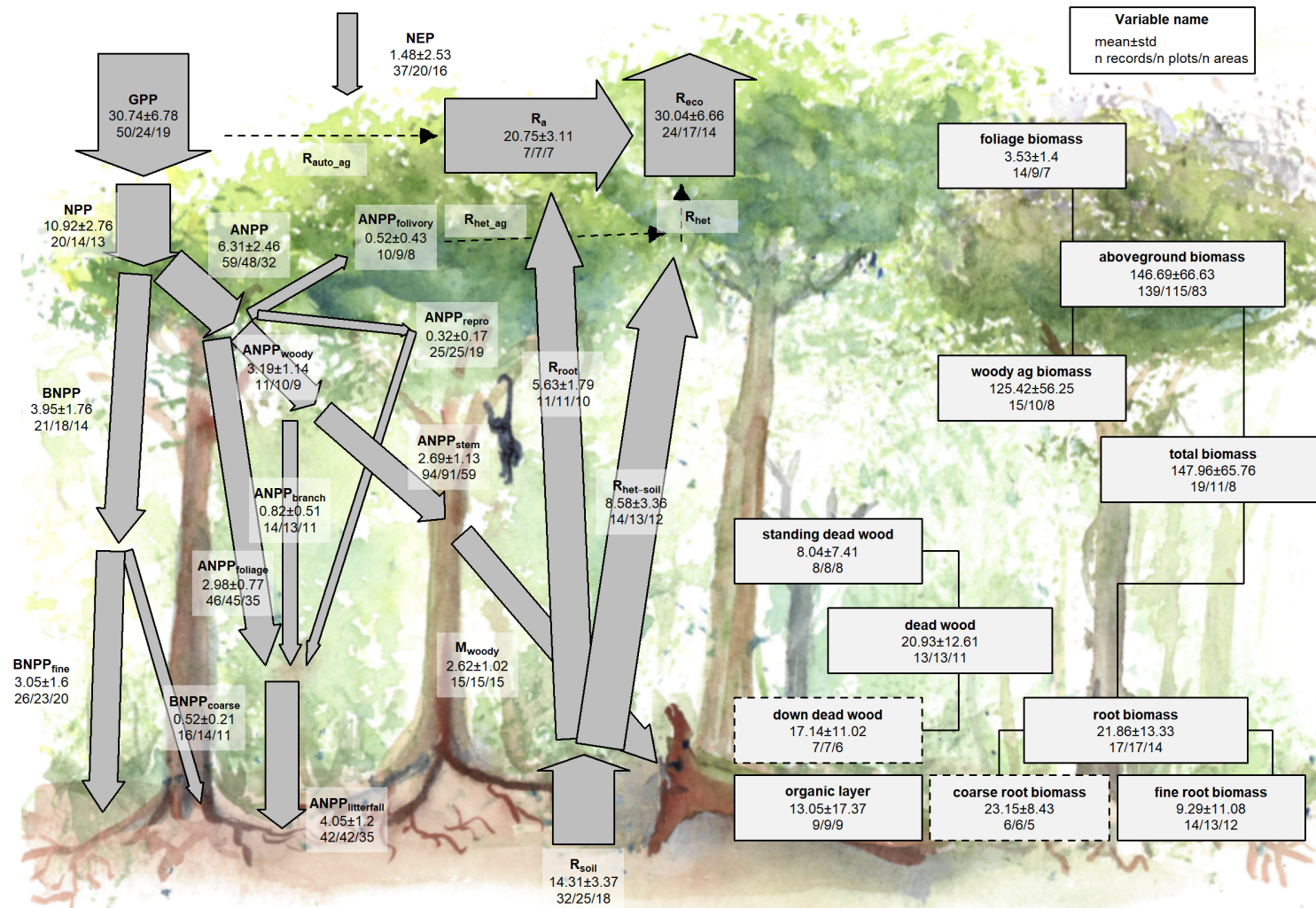


Figure 2 | C cycle diagram for mature tropical broadleaf forests. Arrows indicate fluxes ($\text{Mg C ha}^{-1} \text{ yr}^{-1}$); boxes indicate stocks (Mg C ha^{-1}), with variables as defined in Table 1. Presented are mean \pm std, where geographically distinct areas are treated as the unit of replication. Dashed shape outlines indicate variables with records from <7 distinct geographic areas, and dashed arrows indicate fluxes with no data. To illustrate the magnitude of different fluxes, arrow size is proportional to the square root of corresponding flux. Asterisk after variable name indicates lack of C cycle closure.

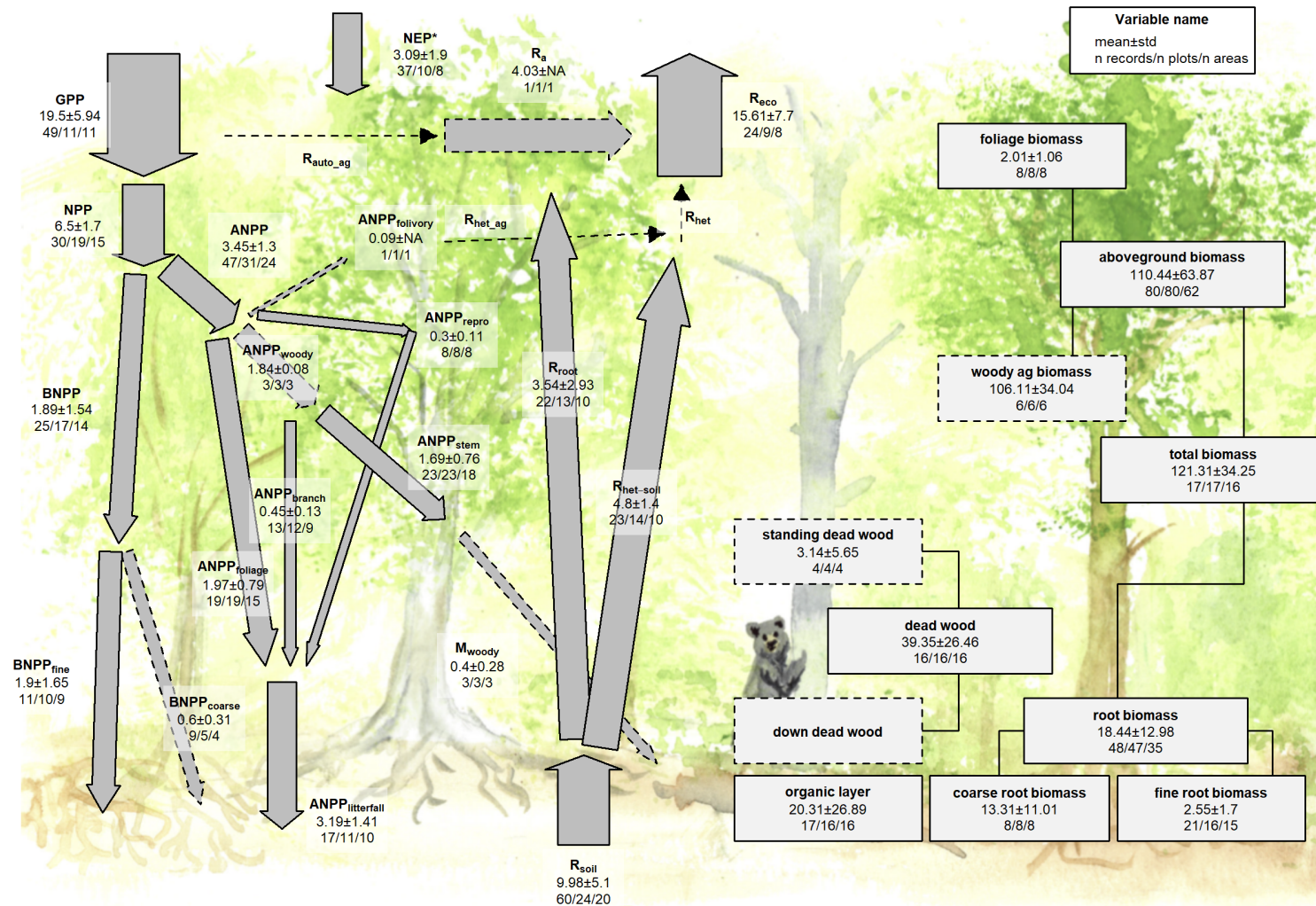


Figure 3 | C cycle diagram for mature temperate broadleaf forests. Arrows indicate fluxes ($\text{Mg C ha}^{-1} \text{ yr}^{-1}$); boxes indicate stocks (Mg C ha^{-1}), with variables as defined in Table 1. Presented are mean \pm std, where geographically distinct areas are treated as the unit of replication. Dashed shape outlines indicate variables with records from <7 distinct geographic areas, and dashed arrows indicate fluxes with no data. To illustrate the magnitude of different fluxes, arrow size is proportional to the square root of corresponding flux. Asterisk after variable name indicates lack of C cycle closure.

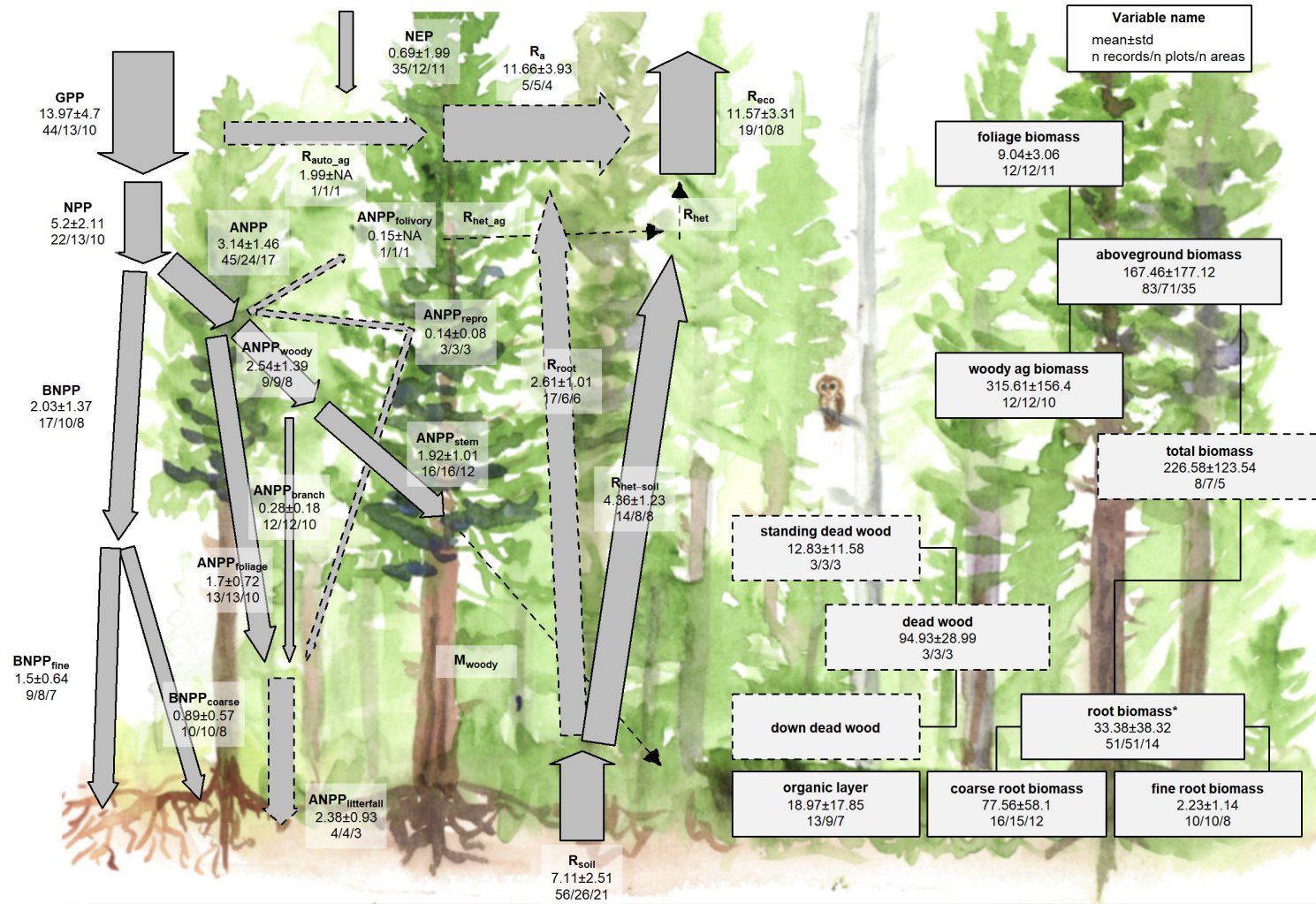


Figure 4 | C cycle diagram for mature temperate conifer forests. Arrows indicate fluxes ($\text{Mg C ha}^{-1} \text{ yr}^{-1}$); boxes indicate stocks (Mg C ha^{-1}), with variables as defined in Table 1. Presented are mean \pm std, where geographically distinct areas are treated as the unit of replication. Dashed shape outlines indicate variables with records from <7 distinct geographic areas, and dashed arrows indicate fluxes with no data. To illustrate the magnitude of different fluxes, arrow size is proportional to the square root of corresponding flux. Asterisk after variable name indicates lack of C cycle closure.

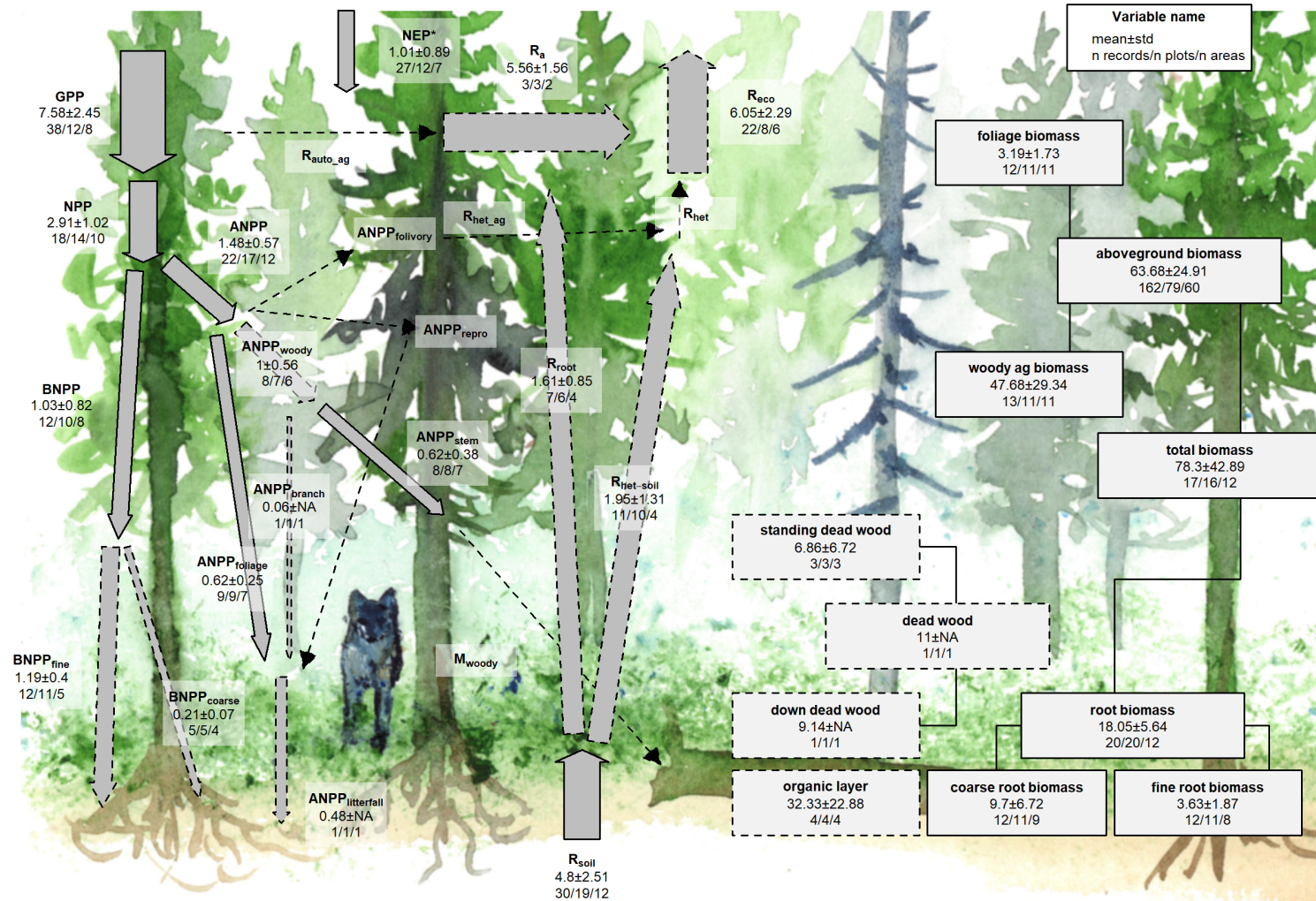


Figure 5 | C cycle diagram for mature boreal conifer forests. Arrows indicate fluxes ($\text{Mg C ha}^{-1} \text{ yr}^{-1}$); boxes indicate stocks (Mg C ha^{-1}), with variables as defined in Table 1. Presented are mean \pm std, where geographically distinct areas are treated as the unit of replication. Dashed shape outlines indicate variables with records from <7 distinct geographic areas, and dashed arrows indicate fluxes with no data. To illustrate the magnitude of different fluxes, arrow size is proportional to the square root of corresponding flux. Asterisk after variable name indicates lack of C cycle closure.

248 **check this with final data (based on Table 1):** There were sufficient data to assess mature forest
249 biome differences for **20** flux variables, and significant differences among biomes were detected for **14**
250 variables (Table 1). In all cases—including C fluxes into, within, and out of the ecosystem—C fluxes were
251 highest in tropical forests, intermediate in temperate (broadleaf or conifer) forests, and lowest in boreal
252 forests (Table 1, Figs. 6, S1-S15). Differences between tropical and boreal forests were always significant,
253 with temperate forests intermediate and significantly different from one or both. Fluxes tended to be
254 numerically greater in temperate broadleaf than conifer forests, but the difference was never statistically
255 significant. This pattern held for the following variables: **** GPP , NPP , $ANPP$, $ANPP_{woody}$,**
256 **$ANPP_{stem}$, $ANPP_{branch}$, $ANPP_{foliage}$, $ANPP_{litterfall}$, M_{woody} , $BNPP$, R_{eco} , R_{soil} , and $R_{het-soil}$ **.** For
257 variables without significant differences among biomes, the same general trends applied.

258 The most notable exception to this pattern was NEP , with no significant differences across biomes but with
259 the largest average in temperate broadleaf forests, followed by temperate conifer, boreal, and tropical forests
260 (Figs. 5,S1). Another exception was for $BNPP_{root-coarse}$, where all records came from high-biomass forests
261 in the US Pacific Northwest, resulting in high values for the temperate conifer biome and no significant
262 differences across biomes (Fig. S10).

263 Thus, C cycling rates generally decreased from tropical to temperate to boreal forests, with the important
264 exception in the overall C balance (NEP).

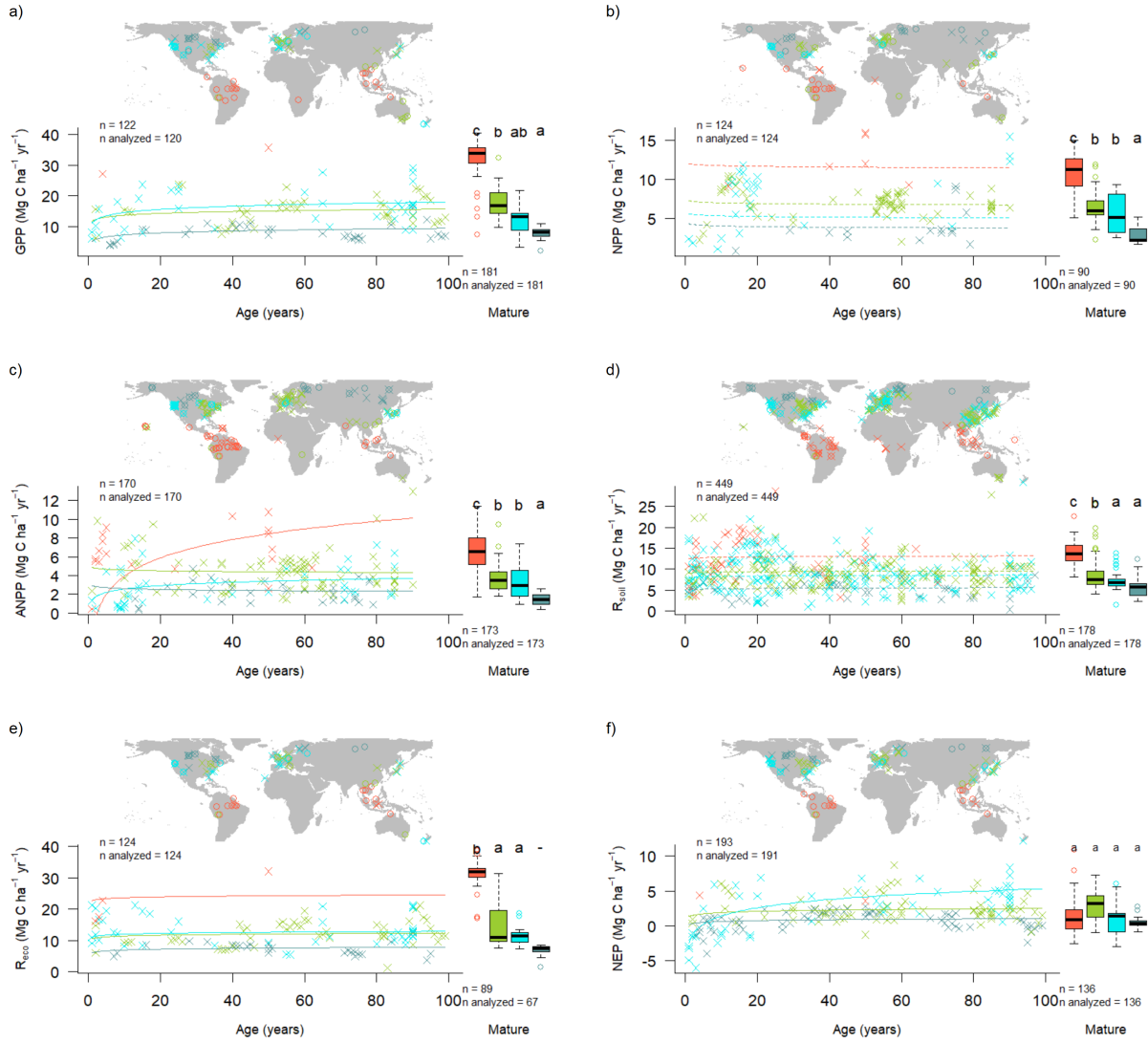


Figure 6 | Age trends and biome differences in some of the major C fluxes: (a) GPP , (b) NPP , (c) $ANPP$, (d) R_{soil} , (e) R_{eco} , and (f) NEP . Map shows data sources (x and o indicate young and mature stands, respectively). In each panel, the left scatterplot shows age trends in forests up to 100 years old, as characterized by a linear mixed effects model with fixed effects of age and biome. The fitted line indicates the effect of age on flux (solid lines: significant at $p < 0.05$, dashed lines: non-significant), and non-parallel lines indicate a significant age \times biome interaction. The boxplot illustrates distribution across mature forests, with different letters indicating significant differences between biomes. Data from biomes that did not meet the sample size criteria (see Methods) are plotted, but lack regression lines (young forests) or test of differences across biomes (mature forests). Individual figures for each flux with sufficient data are given in the Supplement (Figs. S1-S15).

265 **check this with final data (based on Table 1):** There were sufficient data to assess mature forest
 266 biome differences for **9** stock variables, and significant differences among biomes were detected for **6** variables
 267 (B_{tot} , B_{ag} , $B_{ag-wood}$, $B_{foliage}$, $B_{root-coarse}$, DW_{tot} ; Table 1). C stocks had less consistent patterns across
 268 biomes (Figs. 7, S16-S26). In **four of the six** cases (B_{tot} , $B_{ag-wood}$, $B_{root-coarse}$, DW_{tot}), temperate
 269 conifer forests had significantly higher stocks than the other biomes, and boreal forests in the lowest, with
 270 tropical and temperate broadleaf forests in between. For B_{ag} , which had by far the highest sample size,
 271 tropical forests exceeded temperate conifer forests (but not significantly). For $B_{foliage}$, temperate broadleaf
 272 forests were lowest (again, not significantly). The high values for the temperate conifer biome were driven by

273 the very high-biomass forests of the US Pacific Northwest, which are disproportionately represented in the
 274 current version of ForC. Thus, biome differences should be interpreted more as driven more by geographic
 275 distribution of sampling than by true differences.

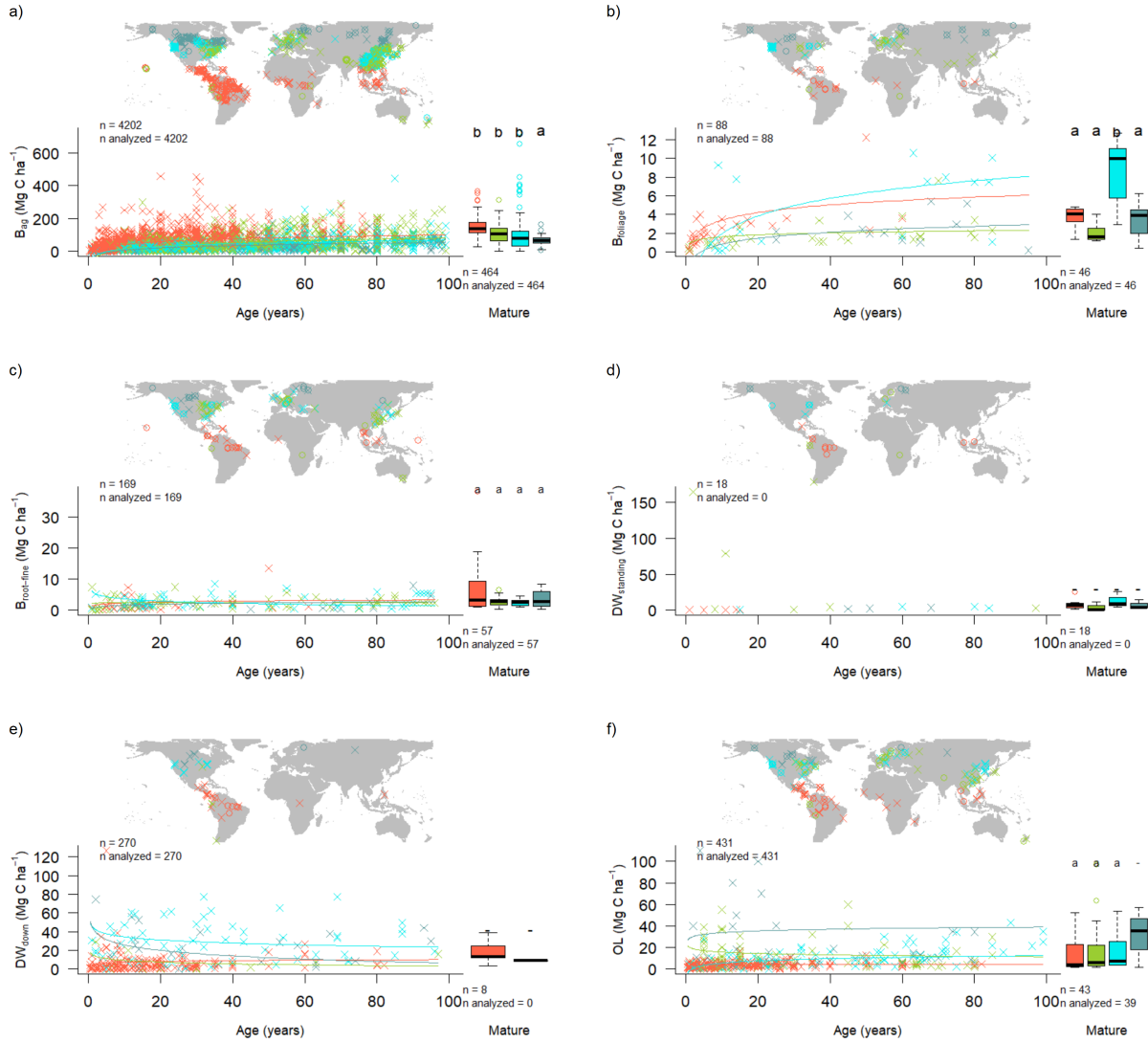


Figure 7 | Age trends and biome differences in some of the major forest C stocks: (a) aboveground biomass, (b) foliage, (c) fine roots, (d) dead wood. Map shows data sources (x and o indicate young and mature stands, respectively). In each panel, the left scatterplot shows age trends in forests up to 100 years old, as characterized by a linear mixed effects model with fixed effects of age and biome. The fitted line indicates the effect of age on flux (solid lines: significant at $p < 0.05$, dashed lines: non-significant), and non-parallel lines indicate a significant age x biome interaction. The boxplot illustrates distribution across mature forests, with different letters indicating significant differences between biomes. Data from biomes that did not meet the sample size criteria (see Methods) are plotted, but lack regression lines (young forests) or test of differences across biomes (mature forests). Individual figures for each stock with sufficient data are given in the Supplement (Figs. S16-S26).

276 C cycling in young forests

277 Average C cycles for forests < 100 years old are presented in Figures 8-11.
 278 Both C stocks and fluxes commonly increased significantly with stand age (Tables 1, S2, Figs. 6-11, S1-S26;
 279 detailed below).

280 *ForC* contained 14 flux variables with sufficient data for cross-biome analyses of age trends in regrowth
281 forests (see Methods) (Fig. 6-7 and **S#- SI figures including plots for all variables**). Of these, 9
282 increased significantly with age: *GPP*, *NPP*, *ANPP*, *ANPP_{foliage}*, *ANPP_{woody}*, *ANPP_{woody-stem}*,
283 *BNPP*, *BNPP_{root-fine}*, *R_{eco}*, and net C sequestration (*NEP*). The remaining five—*ANPP_{woody-branch}*,
284 *BNPP_{root-coarse}*, *R_{soil-het}*, and *R_{soil-het}*—displayed no significant relationship to stand age, although all
285 displayed a positive trend.

286 Differences in C fluxes across biomes typically paralleled those observed for mature forests, with C cycling
287 generally most rapid in the tropics and slowest in boreal forests.

288 The single exception was *ANPP_{stem}*, for which temperate broadleaf forests and temperate conifer forests of
289 age >~30 had slightly higher flux rates than tropical forests (*represented by a single chronosequence*).

290 Notably, the trend of tropical > temperate > boreal held for *NEP* in regrowth forests, in contrast to the
291 lack of biome differences in *NEP* for mature forests (Fig. 6).

292 There were only ## flux variables with sufficient data to test for biome x age interactions: *ANPP*,
293 *ANPP_{woody}*, *ANPP_{stem}*, *ANPP_{litterfall}*, and *BNPP* (Table S2). (**more could be added if age trends
294 become significant after outliers are resolved**) For three of these (*ANPP*, *ANPP_{litterfall}*, *BNPP*),
295 the increase in C flux with age was steepest increase in tropical forests, followed by temperate and then
296 boreal forests (Figs S#). Similarly, *ANPP_{woody}* displayed a steeper increase with age in temperate than
297 boreal forests (no tropical data for this variable). In contrast, for *ANPP_{stem}*, tropical and temperate
298 broadleaf forests had the highest flux rates at young ages, but were surpassed by temperate conifer forests
299 between ages 20 and 50 (Fig. S6).

300 (**this needs to be updated with latest data**) In terms of C stocks, 10 variables had sufficient data to
301 test for age trends. Six of these—*total biomass*, *aboveground biomass*, *aboveground woody biomass*, *foliage
302 biomass*, *root biomass*, and *coarse root biomass*—increased significantly with $\log_{10}[\text{stand.age}]$. The
303 remaining four displayed non-significant positive trends: *fine root biomass*, *total dead wood*, *standing dead
304 wood*, and *organic layer*. (*discuss rates of increase*)

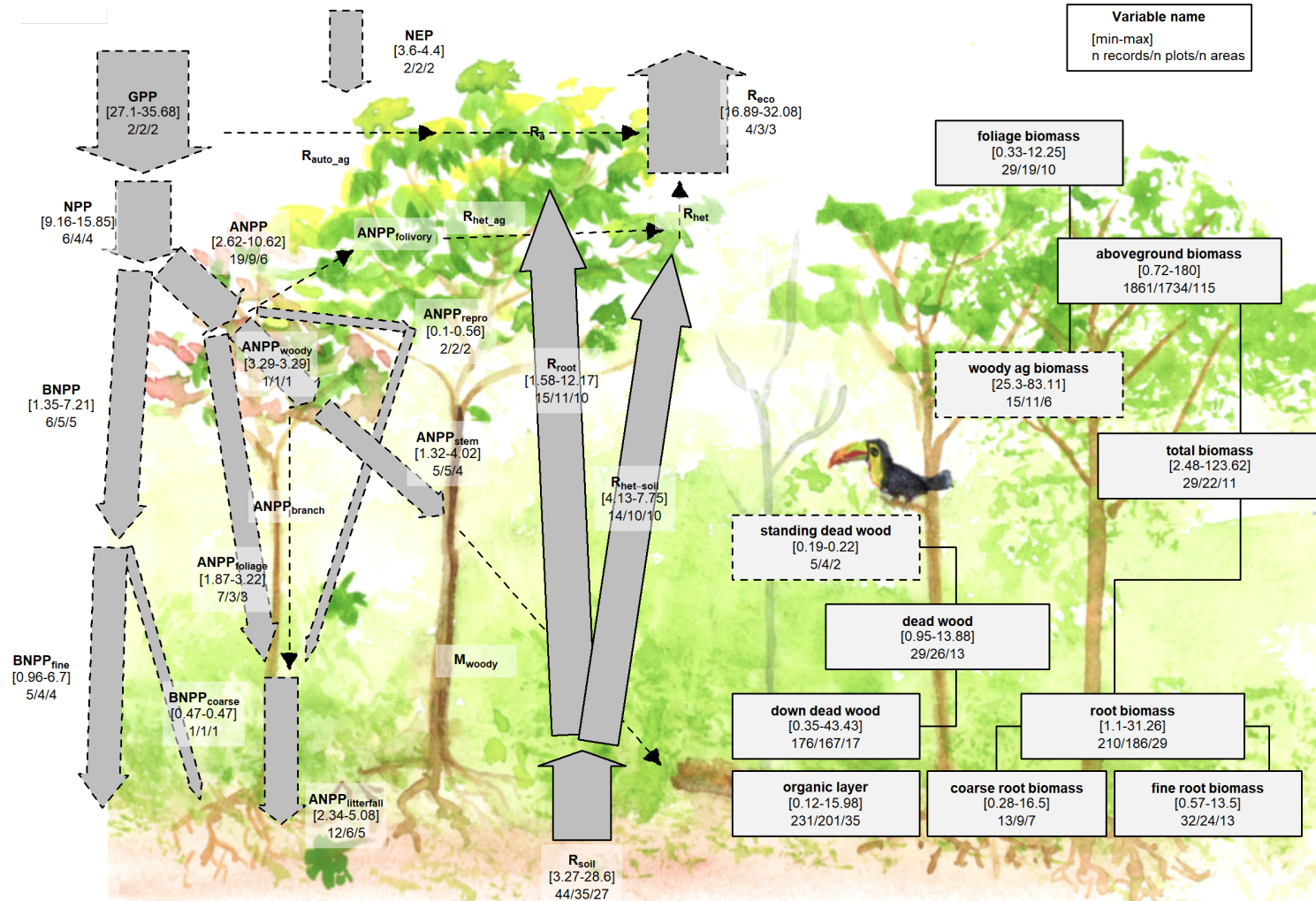


Figure 8 | C cycle diagram for young tropical broadleaf forests. Arrows indicate fluxes ($Mg\ C\ ha^{-1}\ yr^{-1}$); boxes indicate stocks ($Mg\ C\ ha^{-1}$), with variables as defined in Table 1. Presented are observed ranges, where geographically distinct areas are treated as the unit of replication. All units are $Mg\ C\ ha^{-1}\ yr^{-1}$ (fluxes) or $Mg\ C\ ha^{-1}$ (stocks). Dashed shape outlines indicate variables with records from <7 distinct geographic areas, and dashed arrows indicate fluxes with no data. To illustrate the magnitude of different fluxes, arrow size is proportional to the square root of corresponding flux.

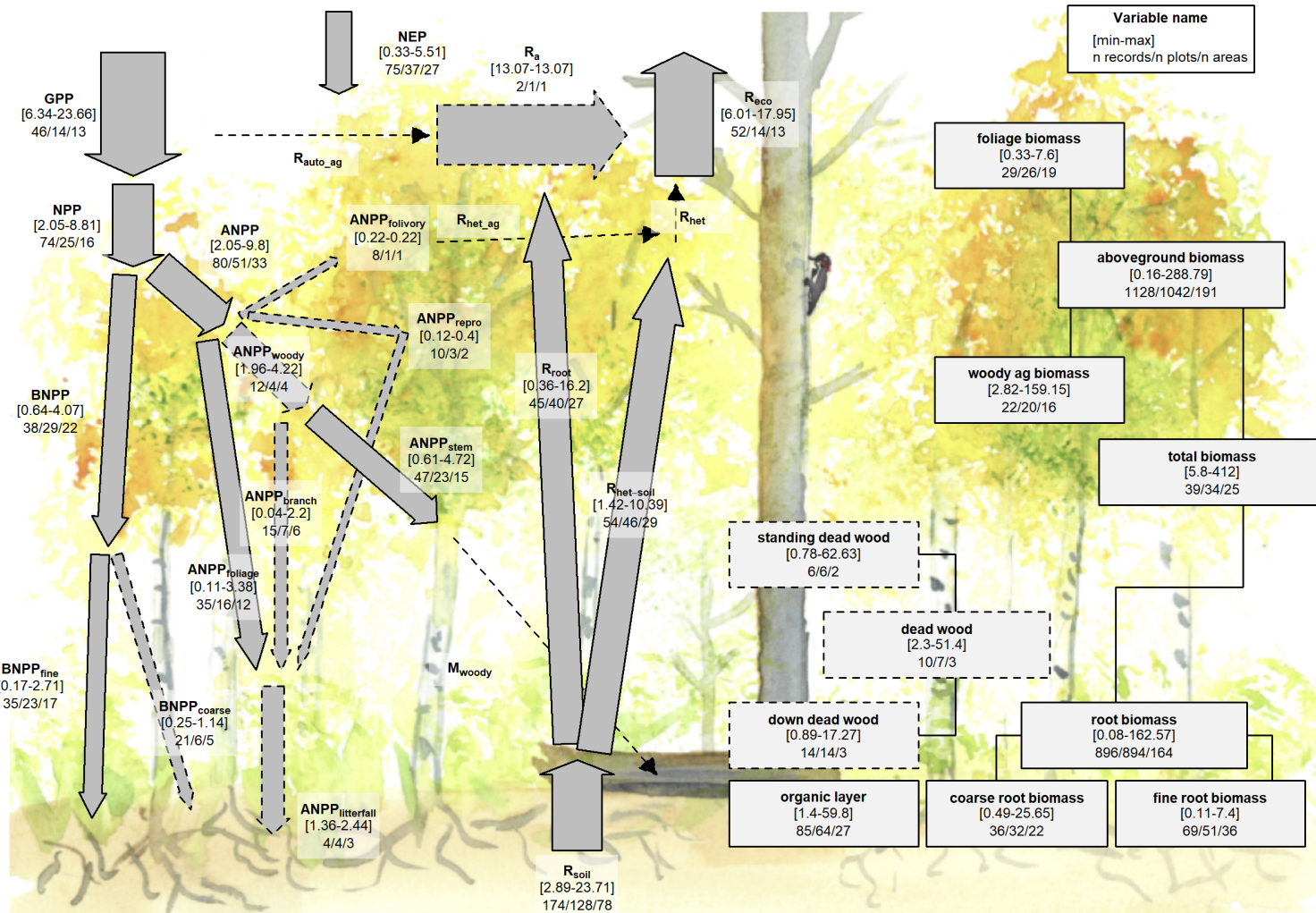


Figure 9 | C cycle diagram for young temperate broadleaf forests. Arrows indicate fluxes ($\text{Mg C ha}^{-1} \text{ yr}^{-1}$); boxes indicate stocks (Mg C ha^{-1}), with variables as defined in Table 1. Presented are observed ranges, where geographically distinct areas are treated as the unit of replication. All units are $\text{Mg C ha}^{-1} \text{ yr}^{-1}$ (fluxes) or Mg C ha^{-1} (stocks). Dashed shape outlines indicate variables with records from <7 distinct geographic areas, and dashed arrows indicate fluxes with no data. To illustrate the magnitude of different fluxes, arrow size is proportional to the square root of corresponding flux.

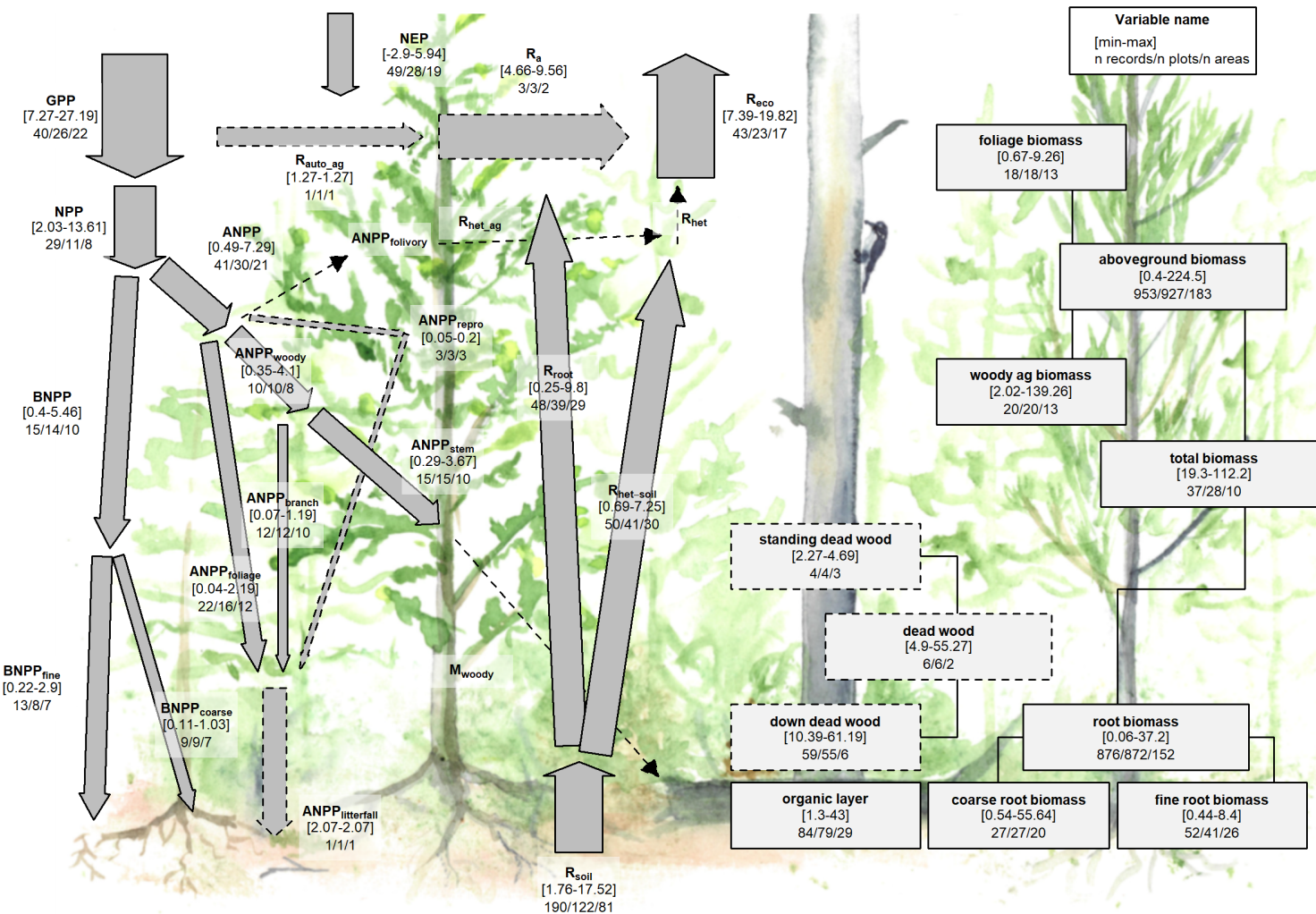


Figure 10 | C cycle diagram for young temperate conifer forests. Arrows indicate fluxes ($\text{Mg C ha}^{-1} \text{ yr}^{-1}$); boxes indicate stocks (Mg C ha^{-1}), with variables as defined in Table 1. Presented are observed ranges, where geographically distinct areas are treated as the unit of replication. All units are $\text{Mg C ha}^{-1} \text{ yr}^{-1}$ (fluxes) or Mg C ha^{-1} (stocks). Dashed shape outlines indicate variables with records from <7 distinct geographic areas, and dashed arrows indicate fluxes with no data. To illustrate the magnitude of different fluxes, arrow size is proportional to the square root of corresponding flux.

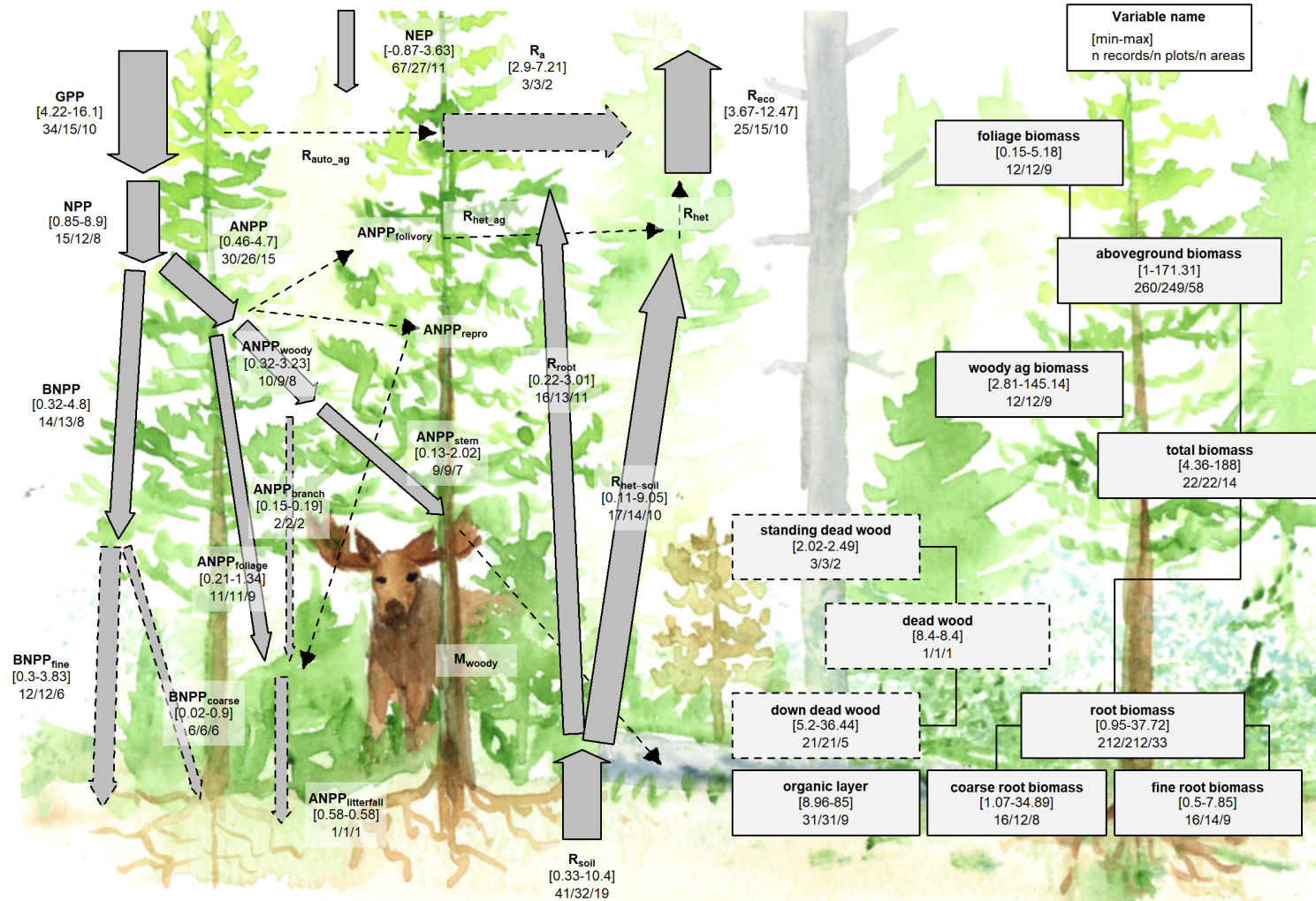


Figure 11 | C cycle diagram for young boreal conifer forests. Arrows indicate fluxes ($Mg\ C\ ha^{-1}\ yr^{-1}$); boxes indicate stocks ($Mg\ C\ ha^{-1}$), with variables as defined in Table 1. Presented are observed ranges, where geographically distinct areas are treated as the unit of replication. All units are $Mg\ C\ ha^{-1}\ yr^{-1}$ (fluxes) or $Mg\ C\ ha^{-1}$ (stocks). Dashed shape outlines indicate variables with records from <7 distinct geographic areas, and dashed arrows indicate fluxes with no data. To illustrate the magnitude of different fluxes, arrow size is proportional to the square root of corresponding flux.

305 **Discussion**

306 *ForC* v3.0 provided unprecedented coverage of most major variables, yielding an internally consistent picture
307 of C cycling in the world's major forest biomes. Carbon cycling rates generally increased from boreal to
308 tropical regions and with stand age. Specifically, the major C fluxes were highest in tropical forests,
309 intermediate in temperate (broadleaf or conifer) forests, and lowest in boreal forests – a pattern that generally
310 held for regrowth as well as mature forests (Figs. 6-7). In contrast to C fluxes, there was little directional
311 variation in mature forest C stocks across biomes (Figs. 2-5, 7). The majority of flux variables, together with
312 most live biomass pools, increased significantly with stand age (Figs. 6-11). Together, these results indicate
313 that, moving from cold to tropical climates and from young to old stands, there is a general acceleration of C
314 cycling, whereas C stocks and *NEP* of mature forests are correlated with a different set of factors.

315 **C variable coverage and budget closure**

316 The large number of C cycle variables covered by *ForC*, and the general consistency between them, provide
317 confidence that our overall reported means provide accurate and useful baselines for analysis (with the
318 caveats that they are unlikely to be accurate representations of C cycling for any particular forest, and that
319 these sample means almost certainly do not represent true biome means).

320 There are of course notable holes in the *ForC* variable coverage, as discussed by Anderson-Teixeira et
321 al. (xxxx), that limit the scope of our inferences here. Notably, *ForC* lacks coverage of fluxes to herbivores
322 and higher consumers, along with the woody mortality and dead wood stocks. Geographically, all variables
323 are poorly covered in Africa and Siberia, a common problem in the carbon-cycle community (Xu and Shang
324 2016 10.1016/j.jplph.2016.08.007, Schimel et al. 2015 10.1073/pnas.1407302112). *ForC* does not include soil
325 carbon, which is covered by other efforts (e.g. Köchy et al. 2015 10.5194/soil-1-351-2015). *ForC* is not
326 intended to replace databases that are specialized for particular parts of the C cycle analyses, e.g.,
327 aboveground biomass (REFS), land-atmosphere fluxes (Baldocchi et al. 2001
328 10.1175/1520-0477(2001)082<2415:FANTTS>2.3.CO;2), soil respiration (Jian et al. 2020
329 10.5194/essd-2020-136), or the human footprint in global forests (Magnani et al. 2007 10.1038/nature05847).

330 In this analysis, the C cycle budgets for mature forests (Figs. 2-5) generally “close”—that is, the sums of
331 component variables do not differ from the larger fluxes by more than one standard deviation. On the one
332 hand, this reflects the general fact that ecosystem-scale measurements tend to close the C budget more easily
333 and consistently than, for example, for energy balance (Stoy et al. 2013 10.1016/j.agrformet.2012.11.004). On
334 the other, however, as noted above *ForC* derives data from multiple heterogeneous sources, often with large
335 errors (standard deviations); as a result, the standard for C closure is relatively loose (cf Houghton 2020
336 10.1111/gcb.15050). Nonetheless, the lack of closure, in the few instances where it occurs, is probably more
337 reflective of differences in the representation of forest types (e.g., disproportionate representation of US
338 Pacific NW for aboveground woody biomass relative to AGB; Fig. 4) than of methodological accuracy. The
339 overall high degree of closure implies that *ForC* gives a consistent picture of C cycling within biomes. This is
340 an important and useful test, because it allows for consistency checks within the C cycle, for example
341 leveraging separate and independently-measured fluxes to constrain errors in another (Phillips et al. 2017
342 10.1007/s11104-016-3084-x, Williams et al. 2014 10.1016/j.rse.2013.10.034, Harmon et al. 2011
343 10.1029/2010JG001495), or producing internally consistent global data products (Wang et al. 2018
344 10.5194/gmd-11-3903-2018).

345 **C cycling across biomes**

346 Our analysis reveals a general deceleration of carbon cycling from the tropics to boreal regions. For mature
347 forests, this is consistent with a large body of previous work demonstrating that C fluxes generally decline
348 with latitude (or increase with temperature) on a global scale (e.g., ???, ???, Li and Xiao 2019, Banbury
349 Morgan *et al* n.d.). The consistency with which this occurs across numerous fluxes is not surprising, but has
350 never been simultaneously assessed across such a large number of variables (but see Banbury Morgan *et al*
351 n.d. for nine autotrophic fluxes). Thus, our analysis reveals that carbon cycling is most rapid in the tropics
352 and slowest in boreal regions, including C fluxes into (*GPP*), within (e.g., *NPP* and its components), and
353 out of (e.g., R_{soil} , R_{eco}) the ecosystem.

354 The notable exception to the pattern of fluxes decreasing from tropical to boreal regions is *NEP* (Fig. 6f),
355 which showed no significant differences across biomes. Unlike the other C flux variables, *NEP* does not
356 represent the rapidity with which C cycles through the ecosystem, but is the balance between C
357 sequestration (*GPP*) and respiratory losses (R_{eco}) and represents net CO₂ sequestration (or release) by the
358 ecosystem. *NEP* tends to be relatively small in mature forest stands [(???), **MORE REFS?**; discussed
359 further below], which accumulate carbon slowly relative to younger stands [(???)**; REFS**], if at all (**REFS**).
360 It is therefore unsurprising that there are no pronounced differences across biomes, suggesting that variation
361 in *NEP* of mature forests is controlled less by climate and more by other factors including moderate
362 disturbances (**REFS**) or disequilibrium of R_{soil} relative to C inputs [e.g., in peatlands where anoxic
363 conditions inhibit decomposition; **REFS**].

364 In contrast to the patterns observed for *NEP* in mature stands, *NEP* of stands between 20 and 100 years of
365 age varied across biomes, being lowest in boreal forests, intermediate in temperate broadleaf forests, and
366 highest in temperate conifer forests (with insufficient data to assess tropical forests; Figs. 6f, S1). This is
367 consistent with findings that live biomass accumulation rates (e.g., ΔB_{ag} or ΔB_{tot}) during early secondary
368 succession decrease with latitude [Anderson *et al* (2006); Cook-Patton *et al* (2020); Figs. 7a, S16-S22]. Note,
369 though, that *NEP* includes not only ΔB_{tot} , but also changes in *DW_{tot}*, *OL*, and soil carbon, and biome
370 differences in the accumulation rates of these variables have not been detected, in part because these variables
371 do not consistently increase with stand age [Cook-Patton *et al* (2020); Figs. 7, S23-S26; see discussion below].

372 For regrowth forests, little is known about cross-biome differences in carbon fluxes, and we are not aware of
373 any previous large-scale comparisons of C fluxes that have been limited to regrowth forests [although they're
374 commonly mixed in with mature forests; e.g., **REFS**]. Thus, this analysis was the first to examine flux
375 trends in regrowth forests across biomes. The observed tendency for young forest fluxes to decrease from
376 tropical to boreal regions paralleled patterns in mature forests (Figs. 6, S1-S15), suggesting that regrowth
377 forests follow latitudinal trends in carbon cycling similar to those of mature forests (e.g., Banbury Morgan *et*
378 *al* n.d.). Yet, *data remain sparse, and further work will be required to explore age x climate*
379 *interactions. Nevertheless, our broad-brush overview indicates that C cycling of regrowth forests is not only*
380 *higher in the tropics, parallel to fluxes in mature forests (Banbury Morgan et al n.d.), but also that it*
381 *accelerates more rapidly with stand age in the tropics, consistent with more rapid biomass accumulation.*

382 In contrast to C fluxes and biomass accumulation rates in regrowth forests, stocks showed less systematic
383 variation across biomes. For aboveground biomass, this Patterns are consistent with others studies showing
384 that variation in forest biomass across broad climatic gradients is modest and constrained more by moisture
385 than temperature (???). (???), using spaceborne lidar, showed a decline in aboveground biomass (all forests,

386 including secondary) with latitude in the N hemisphere, but values exceeding tropical forests in coastal
387 climates of both the southern and northern hemisphere. Highest biomass forests are found in temperate
388 oceanic climates (REF- , something in GEB, some global forest C map) (???). Lack of synthesis comparing
389 deadwood and organic layer across biomes, but see Cook-Patton *et al* (2020) for age trends.
390 Thus, biome differences should be interpreted more as driven more by geographic distribution of sampling
391 than by true differences.

392 Age trends in C cycling

393 (*Just some rough notes at this point*)

394 A relative dearth of data on C cycling in secondary forests, particularly in the tropics (Anderson-Teixeira et
395 al 2016), is problematic in that almost 2/3 of the world's forests were secondary as of 2010 (FAO 2010),
396 implying an under-filled need to characterize age-related trends in forest C cycling.

397 Moreover, as disturbances increase (???, McDowell *et al* 2020), understanding the carbon dynamics of
398 regrowth forests will be increasingly important.

399 It's also important to understand secondary forest C sequestration to reduce uncertainty regarding the
400 potential for carbon uptake by regrowth forests (???, Cook-Patton *et al* 2020).

401 (discuss NEP well, including) NEP increases with log(age) to 100 -> strongest C sinks are established
402 secondary forests. (But presumably this exact number is an artifact; don't over-emphasize.)

403 Our findings are largely consistent with, but built from a far larger dataset than, those of Pregitzer and
404 Euskirchen (2004 <http://dx.doi.org/10.1111/j.1365-2486.2004.00866.x>), who found that NPP and NEP to be
405 higher in intermediate-aged forests than older forests, and emphasize the importance of forest age at the
406 biome scale. Quickly-changing and age-dependent fluxes were also found in a number of previous syntheses
407 (Amiro *et al*. 2010 10.1029/2010JG001390, Magnani *et al*. 2007 10.1038/nature05847).

408 In contrast to most fluxes, *NEP* is highest at intermediate ages

409 Relevance for climate change prediction and mitigation

410 The future of forest C cycling (???) will shape trends in atmospheric CO₂ and the course of climate change.
411 For a human society seeking to understand and mitigate climate change, the data contained in *ForC* and
412 summarized here can help to meet two major challenges.

413 First, improved representation of forest C cycling in models is essential to improving predictions of the future
414 course of climate change. To ensure that models are giving the right answers for the right reasons, it is
415 important to benchmark against multiple components of the C cycle that are internally consistent with each
416 other. By making tens of thousands of records readily available in standardized format, *ForC* makes it
417 feasible for the modeling community to draw upon these data to benchmark models. Integration of *ForC*
418 with models is a goal (Fer *et al.*, in revision).

419 Second, *ForC* can serve as a pipeline through which forest science can inform forest-based climate change
420 mitigation efforts. Such efforts will be most effective when informed by the best available data, yet it is not
421 feasible for the individuals and organizations designing such efforts to sort through literature, often behind
422 paywalls, with data reported in varying units, terminology, etc. One goal for *ForC* is to serve as a pipeline

423 through which information can flow efficiently from forest researchers to decision-makers working to
424 implement forest conservation strategies at global, national, or landscape scales. This is already happening!
425 *ForC* has already contributed to updating the IPCC guidelines for carbon accounting in forests [IPCC 2019;
426 Requena Suarez *et al* (2019); Rozendaal *et al* in prep], mapping C accumulation potential from natural forest
427 regrowth globally (Cook-Patton *et al* 2020), and informing ecosystem conservation priorities (Goldstein *et al*
428 2020).

429 **ForC can complement remote sensing to provide a comprehensive picture of global forest C**
430 **cycling.** (*here, discuss what is well-covered by remote sensing, where ForC is useful for calibrating remote*
431 *sensing, and what ForC can get that remote sensing can't.*) AGB is the largest stock, and most of the
432 emphasis is on this variable. Remote sensing, with calibration based on high-quality ground-based data
433 (Schepaschenko *et al* 2019, Chave *et al* 2019), is the best approach for mapping forest carbon (REFS).
434 However, it is limited in that it is not associated with stand age and disturbance history, except in recent
435 decades when satellite data can be used to detect forest loss, gain, and some of their dominant drivers
436 (Hansen *et al* 2013, Song *et al* 2018, Curtis *et al* 2018). *ForC* is therefore valuable in defining age-based
437 trajectories in biomass, as in Cook-Patton *et al* (2020).

438 *Remote sensing measurements are increasingly useful for global- or regional-scale estimates of forest GPP*
439 *(???, Li and Xiao 2019), aboveground biomass (B_{ag}) (REFS), woody mortality (i.e., B_{ag} losses to mortality*
440 *M_{woody}) (Clark *et al* 2004, Leitold *et al* 2018), and to some extent net ecosystem exchange (NEP) (REFS).*
441 Other variables, in particular respiration fluxes, cannot be remotely sensed ((??)), and efforts such as the
442 Global Carbon Project (**le quere REF**) and NASA CMS (**citation:**
443 https://carbon.nasa.gov/pdfs/CMS_Phase-1_Report_Final_optimized.pdf but maybe
444 better to cite open literature, one of the papers listed at
445 <https://cmsflux.jpl.nasa.gov/get-data/publication-data-sets>) typically compute them as residuals
446 only. (**Ben, it woudl be particularly helpful if you could flesh this out some more.**)

447 In terms of C stocks, there is a paucity of data on dead wood and organic layer (Pan *et al.* ?). These can be
448 significant. (**Note that we've given a lot of emphasis to dead wood (work by Abby, and also**
449 **Jenny), and as a result this work really advances knowledge of dead wood. We'll want to**
450 **highlight that here.**) (*give some stats/ cite figures*).

451 **Move to data availability statement, or methods?:** We recommend that use of *ForC* data go to the
452 original database, as opposed to using “off-the-shelf” values from this publication. This is because (1) *ForC*
453 is constantly being updated, (2) analyses should be designed to match the application, (3) age equations
454 presented here all fit a single functional form that is not necessarily the best possible for all the variables.
455 As climate change accelerates, understanding and managing the carbon dynamics of forests will be critical to
456 forecasting, mitigation, and adaptation. The C data in *ForC*, as summarized here, will be valuable to these
457 efforts.

458 Acknowledgements

459 All researchers whose data is included in *ForC* and this analysis. Ian McGregor for help with the database.
460 Thanks to Norbert Kunert and [Helene's intern] for helpful input at an earlier phase. A Smithsonian
461 Scholarly Studies grant to KAT and HML. WLS grant to KAT.

462 **Data availability statement**

463 Materials required to fully reproduce these analyses, including data, R scripts, and image files, are archived
464 in Zenodo (DOI: TBD]. Data, scripts, and results presented here are also available through the open-access
465 *ForC* GitHub repository (<https://github.com/forc-db/ForC>), where many will be updated as the database
466 develops.

467 **ORCID iD**

468 Kristina J. Anderson-Teixeira: <https://orcid.org/0000-0001-8461-9713>

469 **References**

- 470 Anderson K J, Allen A P, Gillooly J F and Brown J H 2006 Temperature-dependence of biomass
471 accumulation rates during secondary succession *Ecology Letters* **9** 673–82 Online:
472 <http://www.blackwell-synergy.com/doi/abs/10.1111/j.1461-0248.2006.00914.x>
- 473 Anderson-Teixeira K, Herrmann V, CookPatton, Ferson A and Lister K 2020 Forc-db/GROA: Release with
474 Cook-Patton et al. 2020, Nature. Online: <https://zenodo.org/record/3983644>
- 475 Anderson-Teixeira K J, Davies S J, Bennett A C, Gonzalez-Akre E B, Muller-Landau H C, Joseph Wright S,
476 Abu Salim K, Almeyda Zambrano A M, Alonso A, Baltzer J L, Basset Y, Bourg N A, Broadbent E N,
477 Brockelman W Y, Bunyavejchewin S, Burslem D F R P, Butt N, Cao M, Cardenas D, Chuyong G B, Clay K,
478 Cordell S, Dattaraja H S, Deng X, Detto M, Du X, Duque A, Erikson D L, Ewango C E N, Fischer G A,
479 Fletcher C, Foster R B, Giardina C P, Gilbert G S, Gunatilleke N, Gunatilleke S, Hao Z, Hargrove W W,
480 Hart T B, Hau B C H, He F, Hoffman F M, Howe R W, Hubbell S P, Inman-Narahari F M, Jansen P A,
481 Jiang M, Johnson D J, Kanzaki M, Kassim A R, Kenfack D, Kibet S, Kinnaird M F, Korte L, Kral K,
482 Kumar J, Larson A J, Li Y, Li X, Liu S, Lum S K Y, Lutz J A, Ma K, Maddalena D M, Makana J-R, Malhi
483 Y, Marthews T, Mat Serudin R, McMahon S M, McShea W J, Memiaghe H R, Mi X, Mizuno T, Morecroft
484 M, Myers J A, Novotny V, Oliveira A A de, Ong P S, Orwig D A, Ostertag R, Ouden J den, Parker G G,
485 Phillips R P, Sack L, Sainge M N, Sang W, Sri-ngernyuang K, Sukumar R, Sun I-F, Sungpalee W, Suresh H
486 S, Tan S, Thomas S C, Thomas D W, Thompson J, Turner B L, Uriarte M, Valencia R, et al 2015
487 CTFS-ForestGEO: A worldwide network monitoring forests in an era of global change *Global Change Biology*
488 **21** 528–49 Online: <http://onlinelibrary.wiley.com/doi/10.1111/gcb.12712/abstract>
- 489 Anderson-Teixeira K J, Wang M M H, McGarvey J C, Herrmann V, Tepley A J, Bond-Lamberty B and
490 LeBauer D S 2018 ForC: A global database of forest carbon stocks and fluxes *Ecology* **99** 1507–7 Online:
491 <http://doi.wiley.com/10.1002/ecy.2229>
- 492 Anderson-Teixeira K J, Wang M M H, McGarvey J C and LeBauer D S 2016 Carbon dynamics of mature
493 and regrowth tropical forests derived from a pantropical database (TropForC-db) *Global Change Biology* **22**
494 1690–709 Online: <http://onlinelibrary.wiley.com/doi/10.1111/gcb.13226/abstract>
- 495 Baldocchi D, Falge E, Gu L, Olson R, Hollinger D, Running S, Anthoni P, Bernhofer C, Davis K, Evans R,
496 Fuentes J, Goldstein A, Katul G, Law B, Lee X, Malhi Y, Meyers T, Munger W, Oechel W, Paw K T,
497 Pilegaard K, Schmid H P, Valentini R, Verma S, Vesala T, Wilson K and Wofsy S 2001 FLUXNET: A New
498 Tool to Study the Temporal and Spatial Variability of Ecosystem-Scale Carbon Dioxide, Water Vapor, and

- 499 Energy Flux Densities *Bulletin of the American Meteorological Society* **82** 2415–34 Online:
500 [http://journals.ametsoc.org/doi/abs/10.1175/1520-0477\(2001\)082%3C2415:FANTTS%3E2.3.CO;2](http://journals.ametsoc.org/doi/abs/10.1175/1520-0477(2001)082%3C2415:FANTTS%3E2.3.CO;2)
- 501 Banbury Morgan B, Herrmann V, Kunert N, Bond-Lamberty B, Muller-Landau H C and Anderson-Teixeira
502 K J Global patterns of forest autotrophic carbon fluxes *Global Change Biology*
- 503 Bond-Lamberty B and Thomson A 2010 A global database of soil respiration data *Biogeosciences* **7** 1915–26
504 Online: <http://www.biogeosciences.net/7/1915/2010/>
- 505 Chave J, Davies S J, Phillips O L, Lewis S L, Sist P, Schepaschenko D, Armston J, Baker T R, Coomes D,
506 Disney M, Duncanson L, Héault B, Labrière N, Meyer V, Réjou-Méchain M, Scipal K and Saatchi S 2019
507 Ground Data are Essential for Biomass Remote Sensing Missions *Surveys in Geophysics* **40** 863–80 Online:
508 <https://doi.org/10.1007/s10712-019-09528-w>
- 509 Clark D B, Castro C S, Alvarado L D A and Read J M 2004 Quantifying mortality of tropical rain forest
510 trees using high-spatial-resolution satellite data *Ecology Letters* **7** 52–9 Online:
511 <https://onlinelibrary.wiley.com/doi/abs/10.1046/j.1461-0248.2003.00547.x>
- 512 Cook-Patton S C, Leavitt S M, Gibbs D, Harris N L, Lister K, Anderson-Teixeira K J, Briggs R D, Chazdon
513 R L, Crowther T W, Ellis P W, Griscom H P, Herrmann V, Holl K D, Houghton R A, Larrosa C, Lomax G,
514 Lucas R, Madsen P, Malhi Y, Paquette A, Parker J D, Paul K, Routh D, Roxburgh S, Saatchi S, Hoogen J
515 van den, Walker W S, Wheeler C E, Wood S A, Xu L and Griscom B W 2020 Mapping carbon accumulation
516 potential from global natural forest regrowth *Nature* **585** 545–50 Online:
517 <http://www.nature.com/articles/s41586-020-2686-x>
- 518 Curtis P G, Slay C M, Harris N L, Tyukavina A and Hansen M C 2018 Classifying drivers of global forest
519 loss *Science* **361** 1108–11 Online: <http://science.sciencemag.org/content/361/6407/1108>
- 520 Goldstein A, Turner W R, Spawn S A, Anderson-Teixeira K J, Cook-Patton S, Fargione J, Gibbs H K,
521 Griscom B, Hewson J H, Howard J F, Ledezma J C, Page S, Koh L P, Rockström J, Sanderman J and Hole
522 D G 2020 Protecting irrecoverable carbon in Earth's ecosystems *Nature Climate Change* 1–9 Online:
523 <http://www.nature.com/articles/s41558-020-0738-8>
- 524 Grassi G, House J, Dentener F, Federici S, Elzen M den and Penman J 2017 The key role of forests in
525 meeting climate targets requires science for credible mitigation *Nature Climate Change* **7** 220–6 Online:
526 <https://www.nature.com/articles/nclimate3227>
- 527 Griscom B W, Adams J, Ellis P W, Houghton R A, Lomax G, Miteva D A, Schlesinger W H, Shoch D,
528 Siikamäki J V, Smith P, Woodbury P, Zganjar C, Blackman A, Campari J, Conant R T, Delgado C, Elias P,
529 Gopalakrishna T, Hamsik M R, Herrero M, Kiesecker J, Landis E, Laestadius L, Leavitt S M, Minnemeyer S,
530 Polasky S, Potapov P, Putz F E, Sanderman J, Silvius M, Wollenberg E and Fargione J 2017 Natural climate
531 solutions *Proceedings of the National Academy of Sciences* **114** 11645–50 Online:
532 <http://www.pnas.org/lookup/doi/10.1073/pnas.1710465114>
- 533 Hansen M C, Potapov P V, Moore R, Hancher M, Turubanova S A, Tyukavina A, Thau D, Stehman S V,
534 Goetz S J, Loveland T R, Kommareddy A, Egorov A, Chini L, Justice C O and Townshend J R G 2013
535 High-Resolution Global Maps of 21st-Century Forest Cover Change *Science* **342** 850–3 Online:
536 <http://www.sciencemag.org/cgi/doi/10.1126/science.1244693>
- 537 Johnson D J, Needham J, Xu C, Massoud E C, Davies S J, Anderson-Teixeira K J, Bunyavejchewin S,

- 538 Chambers J Q, Chang-Yang C-H, Chiang J-M, Chuyong G B, Condit R, Cordell S, Fletcher C, Giardina C P,
 539 Giambelluca T W, Gunatilleke N, Gunatilleke S, Hsieh C-F, Hubbell S, Inman-Narahari F, Kassim A R,
 540 Katabuchi M, Kenfack D, Litton C M, Lum S, Mohamad M, Nasardin M, Ong P S, Ostertag R, Sack L,
 541 Swenson N G, Sun I F, Tan S, Thomas D W, Thompson J, Umaña M N, Uriarte M, Valencia R, Yap S,
 542 Zimmerman J, McDowell N G and McMahon S M 2018 Climate sensitive size-dependent survival in tropical
 543 trees *Nature Ecology & Evolution* **2** 1436–42 Online: <http://www.nature.com/articles/s41559-018-0626-z>
 544 Krause A, Pugh T A M, Bayer A D, Li W, Leung F, Bondeau A, Doelman J C, Humpenöder F, Anthoni P,
 545 Bodirsky B L, Ciais P, Müller C, Murray-Tortarolo G, Olin S, Popp A, Sitch S, Stehfest E and Arneth A
 546 2018 Large uncertainty in carbon uptake potential of land-based climate-change mitigation efforts *Global
 547 Change Biology* **24** 3025–38 Online: <https://onlinelibrary.wiley.com/doi/abs/10.1111/gcb.14144>
 548 Leitold V, Morton D C, Longo M, dos-Santos M N, Keller M and Scaranello M 2018 El Niño drought
 549 increased canopy turnover in Amazon forests *New Phytologist* **219** 959–71 Online:
 550 <http://doi.wiley.com/10.1111/nph.15110>
 551 Li X and Xiao J 2019 Mapping Photosynthesis Solely from Solar-Induced Chlorophyll Fluorescence: A
 552 Global, Fine-Resolution Dataset of Gross Primary Production Derived from OCO-2 *Remote Sensing* **11** 2563
 553 Online: <https://www.mdpi.com/2072-4292/11/21/2563>
 554 Lutz J A, Furniss T J, Johnson D J, Davies S J, Allen D, Alonso A, Anderson-Teixeira K J, Andrade A,
 555 Baltzer J, Becker K M L, Blomdahl E M, Bourg N A, Bunyavejchewin S, Burslem D F R P, Cansler C A,
 556 Cao K, Cao M, Cárdenas D, Chang L-W, Chao K-J, Chao W-C, Chiang J-M, Chu C, Chuyong G B, Clay K,
 557 Condit R, Cordell S, Dattaraja H S, Duque A, Ewango C E N, Fischer G A, Fletcher C, Freund J A,
 558 Giardina C, Germain S J, Gilbert G S, Hao Z, Hart T, Hau B C H, He F, Hector A, Howe R W, Hsieh C-F,
 559 Hu Y-H, Hubbell S P, Inman-Narahari F M, Itoh A, Janík D, Kassim A R, Kenfack D, Korte L, Král K,
 560 Larson A J, Li Y, Lin Y, Liu S, Lum S, Ma K, Makana J-R, Malhi Y, McMahon S M, McShea W J,
 561 Memiaghe H R, Mi X, Morecroft M, Musili P M, Myers J A, Novotny V, Oliveira A de, Ong P, Orwig D A,
 562 Ostertag R, Parker G G, Patankar R, Phillips R P, Reynolds G, Sack L, Song G-Z M, Su S-H, Sukumar R,
 563 Sun I-F, Suresh H S, Swanson M E, Tan S, Thomas D W, Thompson J, Uriarte M, Valencia R, Vicentini A,
 564 Vrška T, Wang X, Weiblen G D, Wolf A, Wu S-H, Xu H, Yamakura T, Yap S and Zimmerman J K 2018
 565 Global importance of large-diameter trees *Global Ecology and Biogeography* **27** 849–64 Online:
 566 <https://onlinelibrary.wiley.com/doi/abs/10.1111/geb.12747>
 567 Luyssaert S, Inglima I, Jung M, Richardson A D, Reichstein M, Papale D, Piao S L, Schulze E-D, Wingate L,
 568 Matteucci G, Aragao L, Aubinet M, Beer C, Bernhofer C, Black K G, Bonal D, Bonnefond J-M, Chambers J,
 569 Ciais P, Cook B, Davis K J, Dolman A J, Gielen B, Goulden M, Grace J, Granier A, Grelle A, Griffis T,
 570 Grünwald T, Guidolotti G, Hanson P J, Harding R, Hollinger D Y, Hutyra L R, Kolari P, Kruijt B, Kutsch
 571 W, Lagergren F, Laurila T, Law B E, Maire G L, Lindroth A, Loustau D, Malhi Y, Mateus J, Migliavacca M,
 572 Misson L, Montagnani L, Moncrieff J, Moors E, Munger J W, Nikinmaa E, Ollinger S V, Pita G, Rebmann
 573 C, Roupsard O, Saigusa N, Sanz M J, Seufert G, Sierra C, Smith M-L, Tang J, Valentini R, Vesala T and
 574 Janssens I A 2007 CO₂ balance of boreal, temperate, and tropical forests derived from a global database
 575 *Global Change Biology* **13** 2509–37 Online:
 576 <http://onlinelibrary.wiley.com/doi/abs/10.1111/j.1365-2486.2007.01439.x>
 577 McDowell N G, Allen C D, Anderson-Teixeira K, Aukema B H, Bond-Lamberty B, Chini L, Clark J S,
 578 Dietze M, Grossiord C, Hanbury-Brown A, Hurtt G C, Jackson R B, Johnson D J, Kueppers L, Lichstein J

- 579 W, Ogle K, Poulter B, Pugh T A M, Seidl R, Turner M G, Uriarte M, Walker A P and Xu C 2020 Pervasive
580 shifts in forest dynamics in a changing world *Science* **368** Online:
581 <https://science.sciencemag.org/content/368/6494/eaaz9463>
- 582 Pan Y, Birdsey R A, Fang J, Houghton R, Kauppi P E, Kurz W A, Phillips O L, Shvidenko A, Lewis S L,
583 Canadell J G, Ciais P, Jackson R B, Pacala S, McGuire A D, Piao S, Rautiainen A, Sitch S and Hayes D
584 2011 A Large and Persistent Carbon Sink in the World's Forests *Science* **333** 988–93 Online:
585 <http://www.sciencemag.org/content/early/2011/07/27/science.1201609.abstract>
- 586 Pugh T A M, Lindeskog M, Smith B, Poulter B, Arneth A, Haverd V and Calle L 2019 Role of forest
587 regrowth in global carbon sink dynamics *Proceedings of the National Academy of Sciences* **116** 4382–7
588 Online: <http://www.pnas.org/lookup/doi/10.1073/pnas.1810512116>
- 589 Requena Suarez D, Rozendaal D M A, Sy V D, Phillips O L, Alvarez-Dávila E, Anderson-Teixeira K,
590 Araujo-Murakami A, Arroyo L, Baker T R, Bongers F, Brienen R J W, Carter S, Cook-Patton S C,
591 Feldpausch T R, Griscom B W, Harris N, Héault B, Coronado E N H, Leavitt S M, Lewis S L, Marimon B
592 S, Mendoza A M, N'dja J K, N'Guessan A E, Poorter L, Qie L, Rutishauser E, Sist P, Sonké B, Sullivan M J
593 P, Vilanova E, Wang M M H, Martius C and Herold M 2019 Estimating aboveground net biomass change for
594 tropical and subtropical forests: Refinement of IPCC default rates using forest plot data *Global Change
595 Biology* **25** 3609–24 Online: <http://onlinelibrary.wiley.com/doi/abs/10.1111/gcb.14767>
- 596 Schepaschenko D, Chave J, Phillips O L, Lewis S L, Davies S J, Réjou-Méchain M, Sist P, Scipal K, Perger
597 C, Herault B, Labrière N, Hofhansl F, Affum-Baffoe K, Aleinikov A, Alonso A, Amani C, Araujo-Murakami
598 A, Armston J, Arroyo L, Ascarrunz N, Azevedo C, Baker T, Bałazy R, Bedeau C, Berry N, Bilous A M,
599 Bilous S Y, Bissiengou P, Blanc L, Bobkova K S, Braslavskaya T, Brienen R, Burslem D F R P, Condit R,
600 Cuni-Sánchez A, Danilina D, Torres D del C, Derroire G, Descroix L, Sotta E D, d'Oliveira M V N, Dresel C,
601 Erwin T, Evdokimenko M D, Falck J, Feldpausch T R, Foli E G, Foster R, Fritz S, Garcia-Abril A D,
602 Gornov A, Gornova M, Gothard-Bassébé E, Gourlet-Fleury S, Guedes M, Hamer K C, Susanty F H, Higuchi
603 N, Coronado E N H, Hubau W, Hubbell S, Ilstedt U, Ivanov V V, Kanashiro M, Karlsson A, Karminov V N,
604 Killeen T, Koffi J-C K, Konovalova M, Kraxner F, Krejza J, Krisnawati H, Krivobokov L V, Kuznetsov M A,
605 Lakyda I, Lakyda P I, Licona J C, Lucas R M, Lukina N, Lussetti D, Malhi Y, Manzanera J A, Marimon B,
606 Junior B H M, Martinez R V, Martynenko O V, Matsala M, Matyashuk R K, Mazzei L, Memiaghe H,
607 Mendoza C, Mendoza A M, Morozik O V, Mukhortova L, Musa S, Nazimova D I, Okuda T, Oliveira L C,
608 et al 2019 The Forest Observation System, building a global reference dataset for remote sensing of forest
609 biomass *Scientific Data* **6** 1–11 Online: <http://www.nature.com/articles/s41597-019-0196-1>
- 610 Song X-P, Hansen M C, Stehman S V, Potapov P V, Tyukavina A, Vermote E F and Townshend J R 2018
611 Global land change from 1982 to 2016 *Nature* **560** 639–43 Online:
612 <http://www.nature.com/articles/s41586-018-0411-9/>
- 613 Taylor P G, Cleveland C C, Wieder W R, Sullivan B W, Doughty C E, Dobrowski S Z and Townsend A R
614 2017 Temperature and rainfall interact to control carbon cycling in tropical forests ed L Liu *Ecology Letters*
615 **20** 779–88 Online: <http://doi.wiley.com/10.1111/ele.12765>